

SENSORLESS CONTROL OF GRID CONNECTED DOUBLY FED INDUCTION MOTOR DRIVE

A DISSERTATION

*Submitted in partial fulfillment of the
requirements for the award of the degree*

of
MASTER OF TECHNOLOGY
in
WATER RESOURCES DEVELOPMENT

By


ABHINAV SAXENA



**DEPARTMENT OF WATER RESOURCES DEVELOPMENT AND MANAGEMENT
INDIAN INSTITUTE OF TECHNOLOGY ROORKEE
ROORKEE -247 667 (INDIA)
JUNE, 2013**

CERTIFICATE

I hereby certify that the work which is being presented in the thesis entitled, "Sensorless Control of Grid connect doubly fed induction motor drives", in partial fulfillment of the requirements for the award of degree of Master of technology in Water Resources Development in Water Resource Development and Management Department of Indian Institute of technology, Roorkee is an authentic record of my own work carried out under the supervision of Dr. C Thanga Raj (Assist. Professor) WRD&M. The matter in this report has not submitted for award of any other degree of this or any other institution.


Abhinav Saxena

Enrollment no. 11548002

This is to certify that the statement made by the candidate is correct and true to the best of my knowledge.


13/10/13
Dr. C. Thanga Raj

Assistant Professor, WRD&M

Indian Institute of Technology Roorkee

Roorkee

ACKNOWLEDGEMENTS

This thesis entitled as, “Sensorless control of grid connected doubly fed induction motor drive” concludes my work carried out at the Department of Water Resources Development and Management, Indian Institute of Technology Roorkee. The result of work carried out during the the fourth semester of my curriculum whereby I have been accompanied and supported by many people. It is pleasant aspect that I have now the opportunity to express my gratitude for all of them. First of all, I would like to express my gratitude to my supervisor Dr. C. Thanga Raj, Assistant Professor under whose inspiration, encouragement and guidance I have completed my thesis work. I would like to express my thanks to Professor (Dr.) Deepak khare, Head, WRD&M for his time to tome and providing all the facilities in the department during the thesis work. I would like to thanks Prof. S.K Mishra, P.G Coordinator for his excellent guidance and encouragement right from the beginning of this course. I am also thank ful to all faculty and staff members of WRD&M for providing me all the facilities required for the completion of this work. It has a pleasure working at Indian Institute of Technology Roorkee and this is mostly due to the wonderful people who have so journeyed there over the past years. Most importantly, I would like to give God the glory for all the efforts I have put into his work

Abhinav Saxena

M.TECH(Enrollment no. 11548002)

Department of Water Resources Development and Management

ABSTRACT

A simple and implicit sensorless algorithm for estimating the rotor position and speed of the doubly fed induction machine is proposed in this thesis. Instead of computing the stator magnetic flux directly or indirectly, the stator flux vector components in the stationary reference frame are substituted with analytical equivalents in terms of measurable stator and rotor quantities. Thus, it is an implicit estimation process devoid of computing any flux terms and requires only the measured stator voltage and currents in stator and rotor windings apart from knowledge of the machine parameters. It is an open-loop scheme. However, it does not involve integration, recursive techniques, re-computations or programmable low-pass filters etc. Under this scheme, accurate speed measurement, immunity against variation in stator resistance and rotor resistances or in the magnetising inductance are the major advantages of this thesis. Reduced complexity and the computational burden enable the easy implementation of the algorithm on a low-cost fixed point processor. In such high-precision drives, sensor-less control is preferred because of the reduced cabling and hardware complexity, increased reliability, and low maintenance requirements. On the whole, the estimation algorithm is a new vision that holds ability in the area of sensorless control of the DFIM, whether used as a motor or as a generator. Here the discussed electrical system is modeled and simulated in MATLAB/SIMULINK software .

TABLE OF CONTENT:

Topic	Page No.
CERTIFICATE	i
ACKNOWLEDGEMENT	ii
ABSTRACT	iii
TABLE OF CONTENTS	iv
LIST OF FIGURES	vi
LIST OF SYMBOLS	viii
CHAPTER: 1 INTRODUCTION	
1.1 Background	1
1.2 Problem statements	2
1.3 Objectives	2
1.4 Methodology	2
1.5 Scope of dissertation	2
1.6 Significance of the research	3
1.7 Hypothesis	3
CHAPTER:2 DOUBLY FED INDUCTION MACHINE(DFIM)	
2.1 Principle of DFIM	4
2.2 Working of DFIM	5
2.3 Power flow in DFIM	6
2.4 Equivalent circuit diagram of DFIM	7
2.5 Application of DFIM	8
CHAPTER:3 DYNAMIC MODELLING OF DFIM	
3.1 Introduction	9
3.2 Axes transformation	9
3.3 Dynamic modelling of DFIM	12
3.4 dq Model	17

CHAPTER:4	SENSORLESS SCHEME OF DFIM	
4.1	What is sensorless scheme	23
4.2	Sensorless estimation of rotor position and speed	24
4.3	Advantages of sensorless scheme	30
4.4	Applications of sensorless scheme	30
CHAPTER:5	SIMULATION RESULTS	
5.1	Performance of DFIM model under sensorless scheme	31
5.2	Circuit parameters	32
5.3	Various operation of DFIM	32
5.4	Max. error between reference and estimated rotor Speed measurements	34
CHAPTER:6	INDUCTION MOTOR UNDER SENSOR FAULT	
6.1	Introduction	36
6.2	Types of fault injected at speed sensor	36
6.3	Performance evaluations	36
6.4	Conclusion	39
CHAPTER:7	CONCLUSION AND FUTURE SCOPE OF THE WORK	
7.1	Conclusion	41
7.2	Future scope of the work	41
	REFERENCES	43
	APPENDIX	51

LIST OF FIGURES

Figure	Title	Page no.
2.1	Doubly fed induction machine operated In generated mode	5
2.2	Power flow in DFIM	6
2.3	Induction motor equivalent circuit diagram Representing the primary and secondary Winding separately	7
2.4	Conventional induction machine equivalent ckt.	8
2.5	Equivalent ckt. Diagram of DFIM	8
3.1	Transformation of abc to dq axes	10
3.2	Transformation of stationary dq axes to Synchronously rotating frame of dq axes	11
3.3	Ideal 3 phase windings(stator and rotor) of DFIM	12
3.4	DFIM electric equivalent circuit	13
3.5	Space vector principles	15
3.6	Space vector representation in different reference frame	16
3.7	dq model of DFIM in synchronous coordinates	18
3.8	Input-output structure of DFIM simulation block diagram	20
4a	Proposed Sensorless scheme and speed estimation of DFIM	25
4b	Representation of rotor current in different coordinates	25
5.1	Simulation model of Doubly fed induction machine	31
5.3(a)	Performance of machine under subsynchronous speed And comparison of reference and estimated rotor speed	33
5.3(b)	Performance of machine under supersynchronous speed And comparison of reference and estimated rotor speed	34
6.1	No load performance of induction motor drive under Omission fault injected at t=5 sec	37

6.2	Half load performance of induction motor drive under Omission fault injected at $t=5$ sec	38
6.3	Full load performance of induction motor drive under Omission fault injected at $t=5$ sec	38
6.4	Half load performance of induction motor drive under gain fault injected at $t=5$ sec	39



LIST OF SYMBOLS USED:

v_s	stator voltage
i_s	stator current
v_r	rotor voltage
i_r	rotor current
Φ_s	stator flux
ϵ	angle between stator and rotor axis
μ	angle between stationary axis and stator flux axis
θ_1	angle between i_r and stationary axis
θ_2	angle between i_r and rotor axis
ω_e	angular velocity of rotating flux
ω_r	reference angular velocity of rotor
$\omega_r(\text{est})$	estimated angular velocity of rotor
Ψ_{ds}	stator flux in d axis
Ψ_{qs}	stator flux in q axis
Ψ_{dr}	rotor flux in d axis
Ψ_{qr}	rotor flux in q axis

Second subscripts

a, b, c	three phases
a, b	stator reference frame
$_a, _b$	rotor reference frame
d, q	synchronous reference frame

Superscripts

*	reference
---	-----------

CHAPTER: 1

INTRODUCTION

1.1 BACKGROUND

The increasing concern towards environment and fast depleting conventional resources have moved the interest of the researchers towards rationalizing the use of non renewable energy resources and exploring the renewable energy resources to meet the ever-increasing energy demand. A number of renewable energy sources like small hydro, wind, solar, geothermal, etc. are explored[1]. Since small hydro and wind energy sources are available in adequate amount, their utilisation is felt reasonably promising to accomplish the need of future energy[2]. Harnessing mini-hydro and wind energy for electric power generation is an area of research interest and at present, the focus is being given to the effective utilization of these energy resources for quality and reliable power supply[4]. Doubly fed Induction generators are often used in Wind turbines and some micro hydro installations due to their ability to produce valuable power at varying speeds. Electric motors for variable speed drives have been widely used in many industrial applications. In the early years dc motors were widely used for adjustable speed drives because of their ease of control[2]. However, due to advances in both digital technology and power semiconductor devices, ac drives have become more economical and popular. For accurate torque control and precise operating speeds, more sophisticated techniques are necessary in the control of ac motors. These techniques employ high speed Digital Signal processors and control techniques based on estimation or identification of speed and other machine states.

Speed estimation is an important issue of particular interest with respect to Doubly fed induction motor drives as the rotor speed is different from the speed of the revolving magnetic field[19]. The measurement of rotor speed in adjustable speed drives is done using electromagnetic speed transducers. The electromagnetic speed transducers experience errors in speed detection as it is mounted on shaft, some unpleasant vibration produces which shows how they are generally the least reliable drive component[24]. Therefore sensorless speed detection is highly desirable.

1.2 PROBLEM STATEMENT

Commercially available speed measurement devices like any speed transducer require direct contact with the shaft of the Doubly fed induction motor and are often inaccurate and unreliable, Produce fluctuation in grid voltage and frequency after prolonged use[5].

1.3 OBJECTIVES

- Investigate speed estimation using techniques that are dependant on machine parameters and rotor currents in different coordinates
- Operate the machine in both subsynchronous and super synchronous mode, for the sensorless speed estimation of DFIM.

1.4 METHODOLOGY

A literary review is undertaken in order to establish the required background, new trends in industry as well as the relevancy, and application of the research. The implementation of sensorless speed estimation of Doubly fed induction machine is carried out using simulation in MATLAB. This DFIM can operate either in motoring mode or generating mode, in both cases speed estimation will be through rotor currents only without the computation of stator and rotor flux. Basically this flux value is substituted in terms of stator and rotor circuit parameters in various reference frame of the rotor currents coordinate. The method and results are deal with in upcoming chapters.

1.5 SCOPE OF THE DISSERTATION

This research dissertation only considers:

- ❖ Use of current sensor for speed estimation of DFIM
- ❖ Three phase supply to stator terminals and rotor is supplied through grid side Convertors and rotor side convertors
- ❖ Estimation of rotor speed with the help of rotor position using rotor currents in different coordinates and circuit parameters without the involvement of stator and rotor flux
- ❖ Operate the machine in both subsynchronous and supersynchronous mode

1.6 SIGNIFICANCE OF THE RESEARCH

Speed measurement is normally accomplished with a tachometer. Some tachometers require direct contact with the shaft of the motor, while others such as photo tachometer and stroboscope tachometer require close proximity to the shaft. Many motors are located in inaccessible locations or are operated in hazardous Environments e.g. motor operated valves in a nuclear plant. In such instances Personal safety may often preclude the monitoring of these motors, even when it otherwise would be desirable. Many motors, even when accessible, do not provide an exposed shaft due to their mounting configurations[3]. For example, many compressors used in air conditioning and refrigeration equipment are coupled to the motors inside a sealed compartment, thus preventing motor speed measurement by all commercially available tachometers. All these problems can be overcome by means of sensorless speed estimation. Sensorless speed estimation permits the speed sensing to be done remotely, even some distance from the motor. All that is needed is access to the motor electric cables[9]. This could even be at the control centre situated remotely. As the proposed technique of sensorless speed estimation is nonintrusive, it is a very safe method.

1.7 HYPOTHESIS

The combination of the machine parameter dependent and machine parameter independent techniques will provide accurate and reliable speed estimation in doubly fed induction motors drive that does not require contact with the rotating shaft.

CHAPTER :2

DOUBLY FED INDUCTION MACHINE

2.1 Principle of DFIM

Doubly fed electric machines are electric motors or electric generators that have windings on both stationary and rotating parts, where both the windings transfer substantial power between shaft and electrical system. Generally the stator winding is directly connected to the three-phase grid and the three-phase rotor winding is fed from the grid through a rotating or static frequency converter. Doubly fed induction machines are typically used in applications that require varying speed of the machine's shaft in a limited range around the synchronous speed ($\pm 30\%$), because the power rating of the frequency converter is reduced correspondingly. Today doubly fed drives are most common variable speed wind turbine concept.

The principle of the DFIM is that rotor windings are connected to the grid by slip rings and back-to-back voltage source converter that controls both the grid and the rotor currents. Thus rotor frequency can be freely differ from the grid frequency (50Hz). By using the converter to control the rotor currents, it is also possible to adjust the active and reactive power fed to the grid from the stator independently of the generator's turning speed. A doubly fed induction machine is a wound-rotor doubly fed electric machine (generating mode) has several advantages over a singly fed induction machine in wind power applications. Firstly, the rotor circuit is controlled by a power electronics converter, as a result induction motor is capable to deliver real power and absorb reactive power while the induction generator is able to deliver both reactive power and real power [14]. This has important consequences for power system stability and allows the machine to support the grid during severe voltage disturbances. Secondly, the control of the rotor voltages and currents enables the induction machine to remain synchronized with the grid while the wind turbine speed varies. A variable speed wind turbine uses the available wind resource more efficiently than a fixed speed wind turbine, particularly during the light wind conditions. Thirdly, cost of the converter is low when compared with other variable speed solutions because only a fraction of the mechanical power, typically 25-30%, is fed to the grid through the converter, the rest is fed to grid directly from the stator.

The efficiency of DFIM in generating mode is very good for the same reason.

2.2 Working of DFIM:

A doubly fed induction machine is basically a typical, wound rotor induction machine with its stator windings directly connected to the grid and its rotor windings connected to the grid and its rotor windings connected to the grid through a converter as shown in fig2.1. In this figure DFIM is operating in generating mode for driving the wind turbine. The AC/DC/AC Converter is divided to two components: the rotor side converter and the grid side converter. These converters are the voltage sourced converters that use force commutated power electronic devices to synthesize an AC Voltage from a DC source. A capacitor is connected on the DC side acts as the DC source. A coupling inductor is used to connect the grid side converter to the grid directly[10]. The three phase rotor winding is connected to the rotor side converter by slip rings and brushes and the three phase stator windings are directly connected to the grid. The control system produces the pitch angle command and the voltage command signals V_r and V_{gc} for the rotor and grid side converters respectively in order to control the power of the wind turbine, DC voltage and reactive power or the voltage at the grid terminals

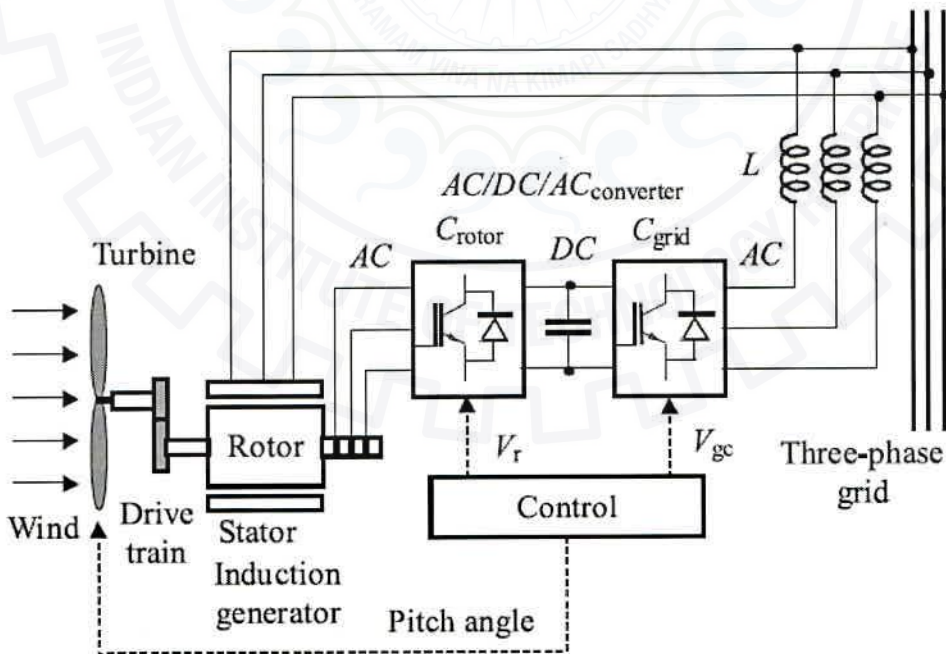


Fig2.1 Doubly fed induction machine operating in generating mode

2.3 Power flow in DFIM:

Fig 2.2 Shows the power flow in DFIM. Generally the absolute value of slip is lower than 1 and consequently the rotor electrical power output P_r is only a fraction of stator real power output P_s . Since the electromagnetic torque T_m is positive for power generation and since W_s is positive and constant for a constant frequency grid voltage, Since P_r is a function of the slip sign and P_r is positive for negative slip (speed greater than synchronous speed) and it is negative for positive slip (speed lower than synchronous speed). For the super synchronous speed operation, rotor power P_r is transmitted to DC bus capacitor and tends to raise the DC voltage. For the sub synchronous speed operation, Rotor power P_r is taken out of the DC bus capacitor and tends to decrease the DC bus voltage[10]. The grid side converter is used to absorb or generate the grid electrical power P_{gc} in order to keep DC voltage remain constant. In steady state for a lossless AC/DC/AC converter P_{gc} is equal to P_r and the speed of the wind turbine is determined by the power P_r absorbed or generated by the rotor side converter[49]. By suitably controlling the rotor side converter, voltage measured at the grid terminals can be controlled by controlling the grid side converter DC bus voltage of the capacitor can be regulated.

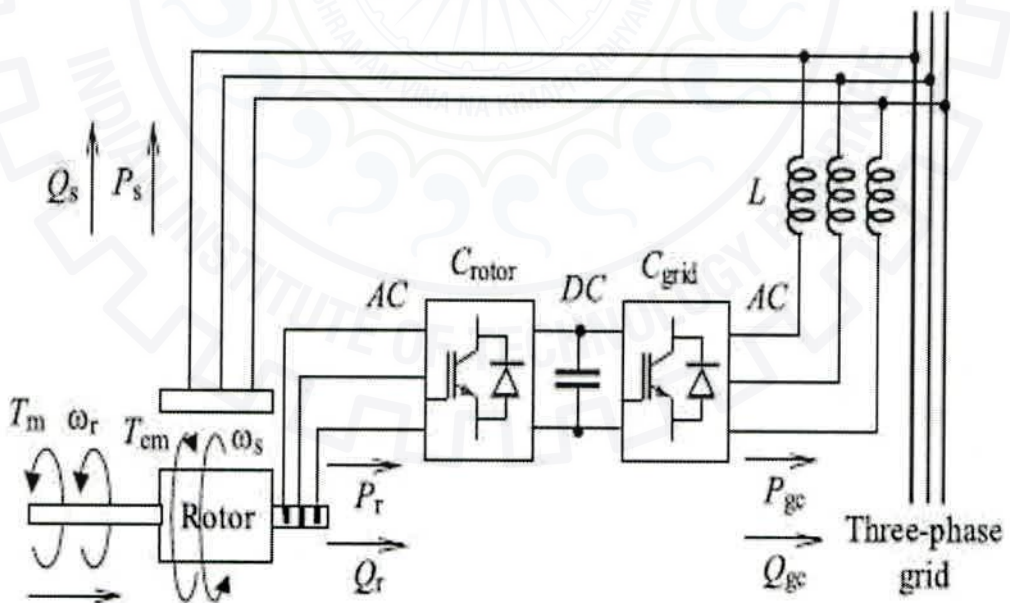


Fig 2.2 Power flow in DFIM

The phase sequence of the AC voltage generated by the rotor side converter is positive for sub synchronous speed and negative for super synchronous speed. The frequency of the voltage generated by rotor side convertor is equal to the product of the grid frequency and the absolute value of the slip. The grid side and the rotor side converter have the capability of absorbing or generating reactive power and could be used to control the reactive power or the voltage at the grid terminals. So, the wind turbine output power and the voltage (reactive power) measured at the grid terminals is controlled by rotor side convertor and grid side converter is used to regulate the voltage of the DC bus capacitor

2.4 Equivalent circuit diagram of DFIM:

The induction machine can be represented by the transformer per phase equivalent circuit model where R_r and X_r represent rotor resistance and reactance referred to the stator side while R_1 and X_1 represent the stator resistance and reactance. The primary internal stator induced voltage E_1 is coupled to the secondary rotor induced voltage E_r by an ideal transformer with an effective turn ratio as shown in fig2.3. But the equivalent circuit of Fig. 2.4 differs from the transformer equivalent circuit primarily in the effects of varying rotor frequency on the rotor voltage E_r [16]. In the case of doubly fed induction machines, there is a voltage injected in the rotor windings so that the normal induction machine equivalent circuit of Fig. 2.4 needs to be modified by adding a rotor injected voltage as shown in Fig.2.5

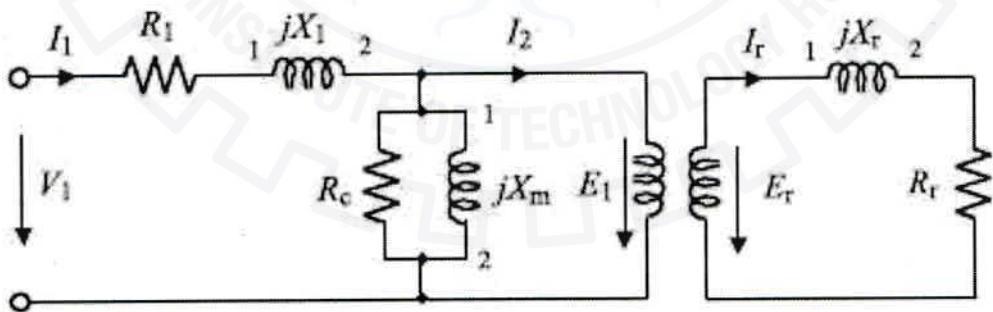


Fig 2.3 Induction motor equivalent circuit diagram representing the primary and secondary windings separately

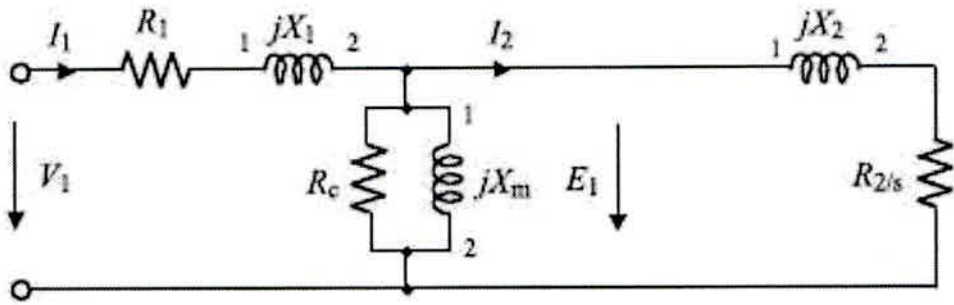


Fig.2.4 Conventional induction machine equivalent circuit

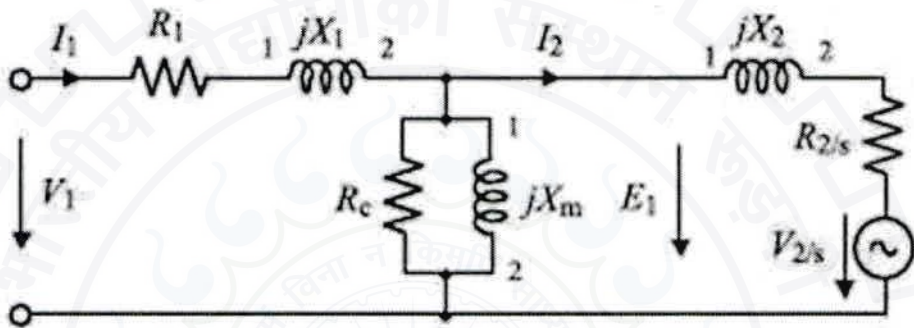


Fig 2.5 Equivalent circuit diagram of DFIM

2.5 Application of DFIM:

- ❖ The main application of DFIM is wind power generation when it is operating in generating mode
- ❖ It can be used in explosive and hazardous environments like mines, contaminated environments, nuclear power plants, underground and underwater applications
- ❖ It can also be used in domestic appliances like air conditioning, refrigerator, conveyor, blower etc.

CHAPTER: 3

DYNAMIC MODELLING OF THE DOUBLY FED INDUCTION MACHINE

3.1 INTRODUCTION

In this chapter, d-q dynamic modeling of the DFIM is presented considering the state of the art related to this field. The dynamic and transient behaviors of the DFIM must be examined for modeling purposes; and perhaps more importantly, for development of the subsequent machine control. This dynamic behaviour explains and defines the behaviour of the machine's variables in transition periods as well as in the steady state. This dynamic behaviour of machines is normally studied by a "dynamic model." By means of the dynamic model it is possible to know at all times the continuous performance (not only at steady state) of the variables of the machine, such as torque, currents, and fluxes, under certain voltage supplying conditions. In this way, by using the information provided by the dynamic model, it is possible to know how the transition from one state to another is going to be achieved, allowing one to detect unsafe behavior's, such as instabilities or high transient currents and also developed control techniques are based on a prediction of the machine's state[21]. On the other hand, the dynamic model provides additional information of the system during the steady state operation, such as dynamic oscillations, torque or current ripples, etc. Thus, this chapter develops d-q dynamic model of the DFIM based on the space vector theory.

3.2 AXES TRANSFORMATION

3.1.1.1 Transformation of three phase stationary to two phase stationary axes [21]

Consider a symmetrical three phase induction machine with stationary a-phase, b-phase and c-phase axes are placed at 120° angle to each other as shown in Fig 3.1. The main aim is to transform the three phase stationary frame variables into two phase

stationary frame variables ($d^s - q^s$) and then transform these to synchronously rotating reference frame variables (d-q), and vice versa.

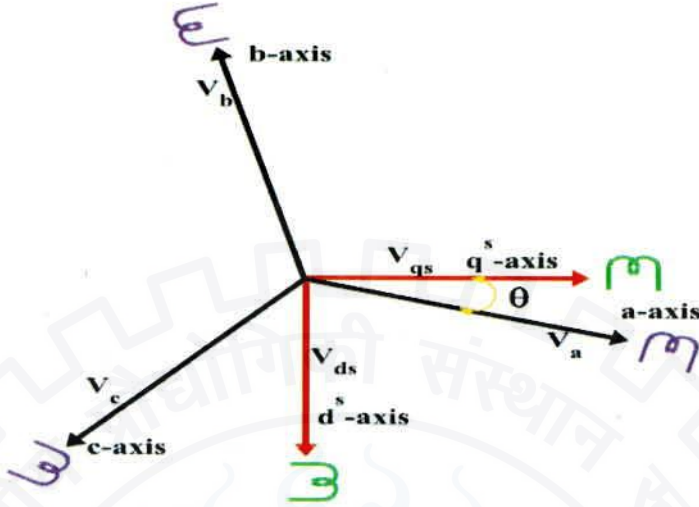


Figure 3.1 Transformation of a-b-c to $d^s - q^s$ axes

Let $d^s - q^s$ axes are oriented at an angle θ from a-b-c axes as shown in Fig 3.1. The voltage (v_{ds}^s and v_{qs}^s) can be resolved into a-b-c components and can be represented in the matrix form as

$$\begin{bmatrix} v_a \\ v_b \\ v_c \end{bmatrix} = \begin{bmatrix} \cos \theta & \sin \theta & 1 \\ \cos(\theta - 120^\circ) & \sin(\theta - 120^\circ) & 1 \\ \cos(\theta + 120^\circ) & \sin(\theta + 120^\circ) & 1 \end{bmatrix} \begin{bmatrix} v_{qs}^s \\ v_{ds}^s \\ v_{0s}^s \end{bmatrix} \quad (3.1)$$

The corresponding inverse relation is

$$\begin{bmatrix} v_{qs}^s \\ v_{ds}^s \\ v_{0s}^s \end{bmatrix} = \frac{2}{3} \begin{bmatrix} \cos \theta & \cos(\theta - 120^\circ) & \cos(\theta + 120^\circ) \\ \sin \theta & \sin(\theta - 120^\circ) & \sin(\theta + 120^\circ) \\ 0.5 & 0.5 & 0.5 \end{bmatrix} \begin{bmatrix} v_a \\ v_b \\ v_c \end{bmatrix} \quad (3.2)$$

Where v_{0s}^s is added as the zero sequence component. Other parameters like current, flux linkages can be transformed by similar manner. It is more convenient to

set $\theta=0^\circ$, so that q-axis is aligned with the a-axis in this case (The alignment of the axes are optional, d-axis can also be aligned with a-axis). The sine components of d and q parameters will be replaced with cosine values, and vice versa if d-axis coincides with a-axis.

3.1.1.2 Transformation of two phase stationary to two phase synchronously rotating axes

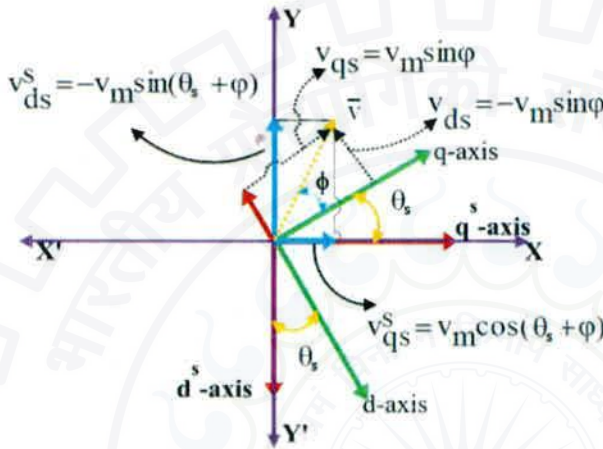


Figure 3.2. Transformation of stationary $d^s - q^s$ axes to synchronously rotating frame d-q axes

Fig 3.2 shows the synchronously rotating d-q axes which rotate at synchronous speed ω_s with respect to $d^s - q^s$ axes. The two phase windings are transformed into the fictitious windings mounted on the d-q axes.

The voltages on the $d^s - q^s$ axes can be converted into d-q axes as follows;

$$v_{qs}^s = v_{qs}^s \cos \theta_s - v_{ds}^s \sin \theta_s \quad (3.3)$$

$$v_{ds}^s = v_{qs}^s \sin \theta_s + v_{ds}^s \cos \theta_s \quad (3.4)$$

Again resolving the rotating frame parameters into a stationary frame the relations are

$$v_{qs}^s = v_{qs} \cos \theta_s + v_{ds} \sin \theta_s \quad (3.5)$$

$$v_{ds}^s = -v_{qs} \sin \theta_s + v_{ds} \cos \theta_s \quad (3.6)$$

3.3 DYNAMIC MODELING OF DFIM

According to models of AC machines developed by several authors and as discussed at the beginning of the previous chapter, the simplified and idealized DFIM model can be described as three windings in the stator and three windings in the rotor, as illustrated in Figure 3.3. These windings are an ideal representation of the real machine, which helps to derive an equivalent electric circuit, as shown in Figure 3.4. Under this idealized model, the instantaneous stator voltages, current, and fluxes of the machine can be described by the following electric equations:

$$v_{as}(t) = R_s i_{as}(t) + \frac{d\psi_{as}(t)}{dt} \quad (3.7)$$

$$v_{bs}(t) = R_s i_{bs}(t) + \frac{d\psi_{bs}(t)}{dt} \quad (3.8)$$

$$v_{cs}(t) = R_s i_{cs}(t) + \frac{d\psi_{cs}(t)}{dt} \quad (3.9)$$

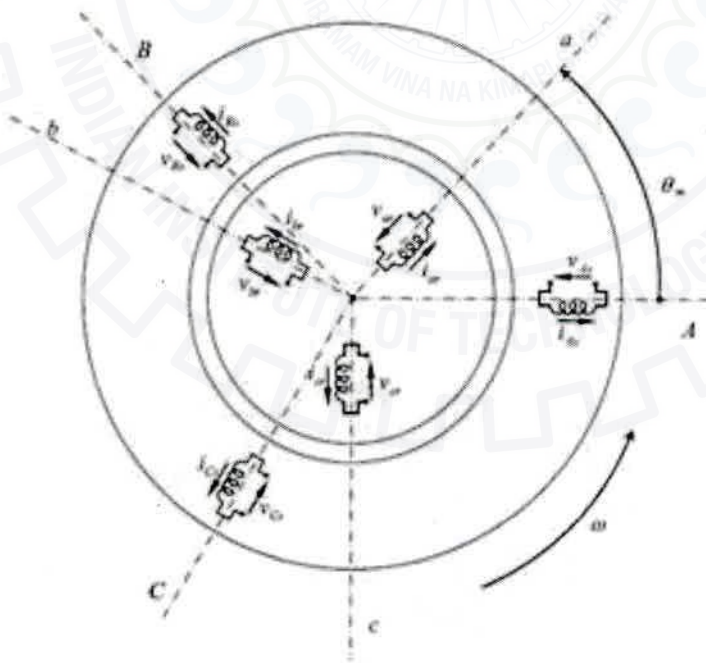


Figure 3.3 Ideal three-phase windings (stator and rotor) of the DFIM. [76]

The DFIM can be modeled by the next equivalent electric circuit [1].

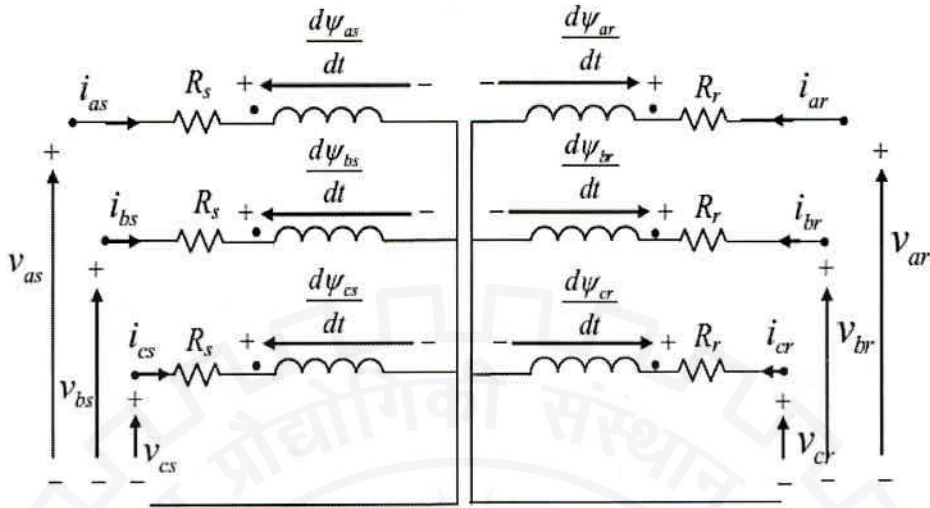


Figure 3.4 DFIM electric equivalent circuit. [74]

where R_s is the stator resistance; $i_{as}(t)$, $i_{bs}(t)$ and $i_{cs}(t)$ are the stator currents of phases a, b, and c; $v_{as}(t)$, $v_{bs}(t)$ and $v_{cs}(t)$ are the applied stator voltages; and $\psi_{as}(t)$, $\psi_{bs}(t)$ and $\psi_{cs}(t)$ are the stator fluxes. The stator side electric magnitudes, at steady state, have a constant sinusoidal angular frequency, ω_s , the angular frequency imposed by the grid.

Similarly, the rotor magnitudes are described by

$$v_{ar}(t) = R_r i_{ar}(t) + \frac{d\psi_{ar}(t)}{dt} \quad (3.10)$$

$$v_{br}(t) = R_r i_{br}(t) + \frac{d\psi_{br}(t)}{dt} \quad (3.11)$$

$$v_{cr}(t) = R_r i_{cr}(t) + \frac{d\psi_{cr}(t)}{dt} \quad (3.12)$$

where R_r is the rotor resistance referred to the stator; $i_{ar}(t)$, $i_{br}(t)$ and $i_{cr}(t)$ are the stator referred rotor currents of phases a, b, and c; $v_{ar}(t)$, $v_{br}(t)$ and $v_{cr}(t)$ are the stator referred rotor voltages; and $\psi_{ar}(t)$, $\psi_{br}(t)$ and $\psi_{cr}(t)$ are the rotor fluxes.

Under steady state operating conditions, the rotor magnitudes have constant angular frequency, ω_r . In this chapter, assuming a general DFIM built with different turns in the stator and rotor, all parameters and magnitudes of the rotor are referred to the stator.

The relation between the stator angular frequency and the rotor angular frequency is

$$\omega_r = \omega_s - \omega_m \quad (3.13)$$

where

ω_r = angular frequency of the voltages and currents of the rotor windings (rad/s)

ω_s = angular frequency of the voltages and currents of the stator windings (rad/s)

ω_m = angular frequency of the rotor (rad/s)

and

$$\omega_m = p\Omega_m \quad (3.14)$$

where

Ω_m = mechanical rotational speed at the rotor (rad/s)

Hence, the rotor variables (voltages, currents, and fluxes) present a pulsation ω_r that varies with the speed. This is graphically shown in the examples of this chapter. For simplicity in the notation, the time dependence of the magnitudes will be omitted in the following sections. In subsequent sections, the magnitudes and parameters of the rotor are always referred to the stator.

3.1.1.3 Space Vector Notation of the DFIM

The space vector notation, is a commonly extended tool to represent the flux, voltage and current magnitudes of the machine in a compact manner. Thus, a three phase magnitude (x_a, x_b and x_c) can be represented by a space vector (\vec{x}_s) as follows [2]:

$$\vec{x}_s = x_a + j \bullet x_b = \frac{2}{3}(x_a + a \bullet x_b + a^2 \bullet x_c) \quad (3.15)$$

$$\text{Where } a = e^{j\frac{2\pi}{3}} \quad (3.16)$$

The constant $2/3$ is chosen to scale the space vectors according to the maximum amplitude of the three phase magnitudes.

The subscript “s” denotes that the space vector is referred to the reference frame of the stator of the DFIM. Added to this, thanks to the space vector notation, the three phase magnitudes may be represented by a rotating space vector, that can also be represented by two phase magnitudes (x_α and x_β) in the real-imaginary plane, as illustrated in Figure 3.5.

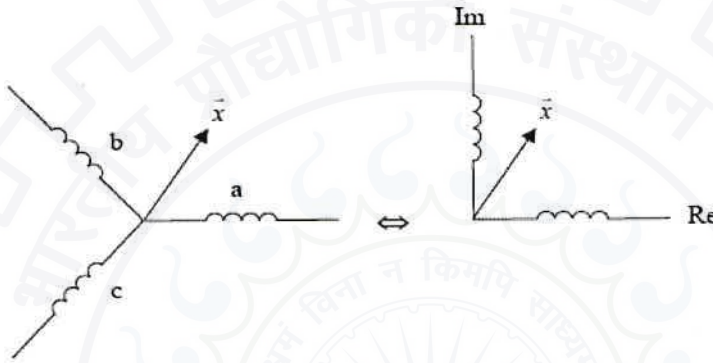


Figure 3.5 Space vector principles.

Hence, in general a space vector can be expressed as:

$$\vec{x}^s = \hat{x} \cdot e^{j(\theta_s + \phi)} \quad (3.17)$$

Where \hat{x} the amplitude, ϕ is the phase shift and θ_s is the rotation position that can be calculated from:

$$\theta_s = \int \omega_s dt \quad (3.18)$$

In general, three different reference frames are used to express the different magnitudes of the DFIM in space vector notation.

1. **The stator reference frame (α - β):** Aligned with the stator, the rotating speed of the frame is zero, and the space vector referenced to it, rotates at the synchronous speed ω_s .
2. **The rotor reference frame (D-Q):** Aligned with the rotor, the rotating speed of the frame is the speed of the rotor ω_m , and the space vector referenced to it rotates



at the slip speed ω_r .

$$\vec{x}^r = x_D + j \cdot x_Q = e^{-j\theta_m} \cdot \vec{x}^s \quad (3.19)$$

Being

$$\theta_m = \int \omega_m dt$$

3. **The synchronous reference frame (d-q):** The rotating speed of the frame is the synchronous speed ω_s , and the space vector referenced to it does not rotate, i.e. it presents constant real and imaginary parts.

$$\vec{x}^a = x_d + j \cdot x_q = e^{-j\theta_s} \cdot \vec{x}^s \quad (3.20)$$

Or

$$\vec{x}^a = x_d + j \cdot x_q = e^{-j\theta_r} \cdot \vec{x}^r \quad (3.22)$$

Being

$$\theta_r = \int \omega_r dt \quad (3.24)$$

And

$$\omega_r = \omega_s - \omega_m \quad (3.25)$$

The different reference frame representations are shown in Figure 3.6.

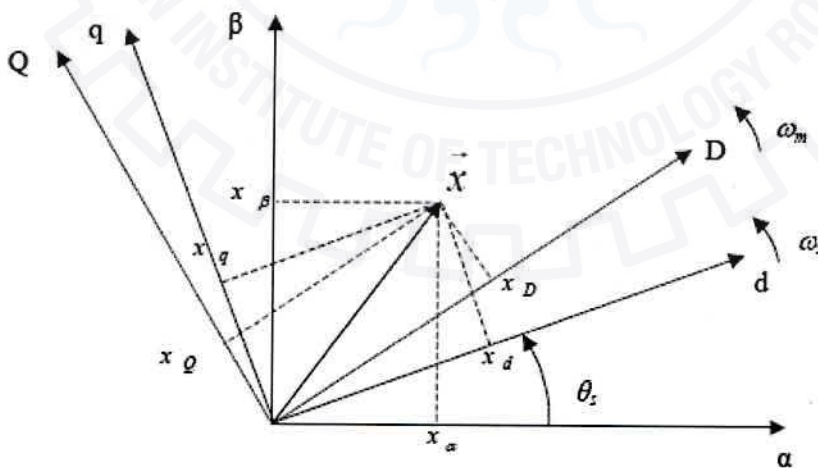


Figure 3.6 Space vector representation in different reference frames. [75]

3.4 dq MODEL

In this subsection, in contrast with the previous subsection, the differential equations representing the model of the DFIM are derived, using the space vector notation in the synchronous reference frame[43].

By multiplying Equations (3.7) and (3.10) by 2/3, then multiplying Equations (3.8) and (3.11) by (2/3)a, and also multiplying Equations (3.9) and (3.12) by (2/3)a², the addition of the resulting equations yields the voltage equations of the DFIM, in space vector form:

$$\vec{v}_s^s = R_s \vec{i}_s^s + \frac{d\vec{\psi}_s^s}{dt} \quad (3.26)$$

$$\vec{v}_r^r = R_r \vec{i}_r^r + \frac{d\vec{\psi}_r^r}{dt} \quad (3.27)$$

Where \vec{v}_s^s is the stator voltage space vector, \vec{i}_s^s is the stator current space vector, and $\vec{\psi}_s^s$ is the stator flux space vector. Equation (4.9) is represented in stator coordinates ($\alpha\beta$ reference frame). \vec{v}_r^r is the rotor voltage space vector, \vec{i}_r^r is the rotor current space vector, and $\vec{\psi}_r^r$ is the rotor flux space vector. Equation (4.10) is represented in rotor coordinates (DQ reference frame).

Note that the superscripts “s” and “r” indicate that space vectors are referred to stator and rotor reference frames, respectively. On the other hand, the correlation between the fluxes and the currents, in space vector notation, is given by

$$\vec{\psi}_s^s = L_s \vec{i}_s^s + L_m \vec{i}_r^s \quad (3.28)$$

$$\vec{\psi}_r^r = L_m \vec{i}_s^r + L_r \vec{i}_r^r \quad (3.29)$$

where L_s and L_r are the stator and rotor inductances, L_m is the magnetizing inductance, and they are related to the stator leakage inductance $L_{\sigma s}$ and the rotor leakage inductance $L_{\sigma r}$, according to the following expressions:

$$L_s = L_{\sigma s} + L_m \quad (3.30)$$

$$L_r = L_{\sigma r} + L_m \quad (3.31)$$

Multiplying equations by $e^{-j\theta_s}$ and $e^{-j\theta_r}$, respectively, the stator and rotor voltage equations yields.

$$\vec{v}_s^a = R_s \vec{i}_s^a + \frac{d\vec{\psi}_s^a}{dt} + j\omega_s \vec{\psi}_s^a \quad (3.32)$$

$$\vec{v}_r^a = R_r \vec{i}_r^a + \frac{d\vec{\psi}_r^a}{dt} + j(\omega_s - \omega_m) \vec{\psi}_r^a \quad (3.33)$$

For the modeling of DFIM in synchronously rotating frame we need to represent the two phase stator ($d_s - q_s$) and rotor ($d_r - q_r$) circuit variables in a synchronously rotating (d-q) frame. Hence, the dq equivalent circuit model of the DFIM, in synchronous coordinates, is represented in Figure 3.7.

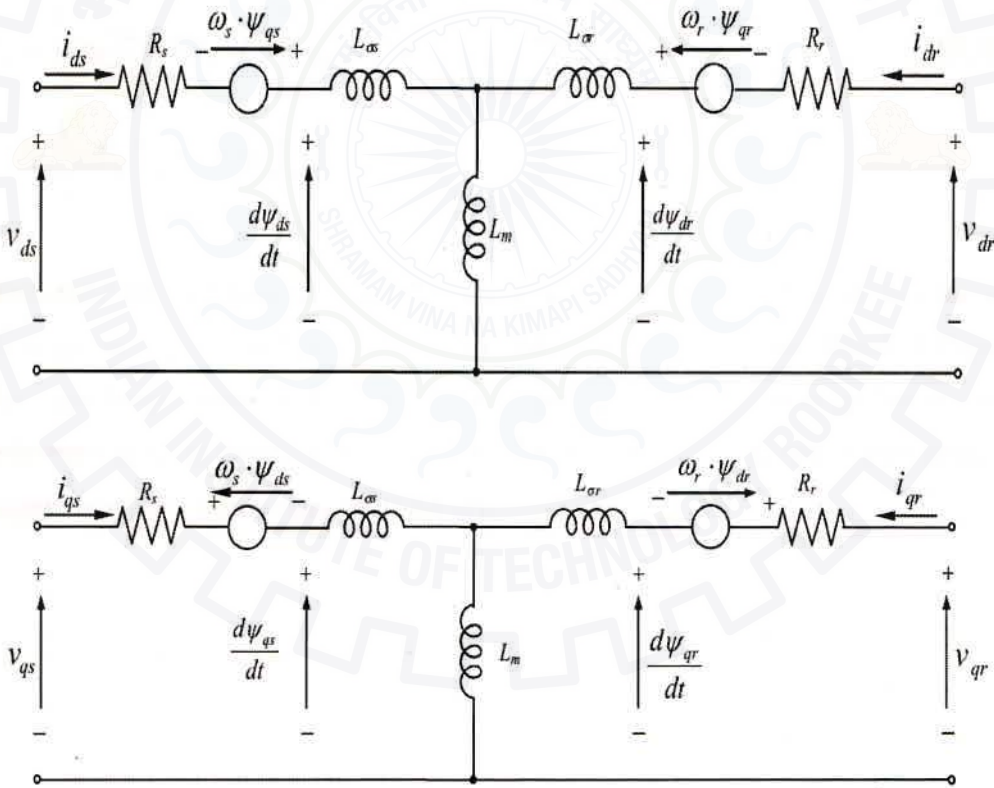


Figure 3.7 dq Model of the DFIM in synchronous coordinates. [75]

Continuing with the model, the electric powers on the stator side and on the rotor side are calculated as follows:

$$P_s = \frac{3}{2} \operatorname{Re} \left\{ \vec{v}_s \cdot \vec{i}_s^* \right\} = \frac{3}{2} (v_{ds} i_{ds} + v_{qs} i_{qs}) \quad (3.34)$$

$$P_r = \frac{3}{2} \operatorname{Re} \left\{ \vec{v}_r \cdot \vec{i}_r^* \right\} = \frac{3}{2} (v_{dr} i_{dr} + v_{qr} i_{qr}) \quad (3.35)$$

$$Q_s = \frac{3}{2} \operatorname{Im} \left\{ \vec{v}_s \cdot \vec{i}_s^* \right\} = \frac{3}{2} (v_{qs} i_{ds} - v_{ds} i_{qs}) \quad (3.36)$$

$$Q_r = \frac{3}{2} \operatorname{Im} \left\{ \vec{v}_r \cdot \vec{i}_r^* \right\} = \frac{3}{2} (v_{qr} i_{dr} - v_{dr} i_{qr}) \quad (3.37)$$

where the superscript * represents the complex conjugate of a space vector as was used in phasors. Finally, the electromagnetic torque can be found from

$$\begin{aligned} T_e &= \frac{3}{2} p \frac{L_m}{L_s} \operatorname{Im} \left\{ \vec{\psi}_s \cdot \vec{i}_r^* \right\} = \frac{3}{2} p \frac{L_m}{L_s} (\Psi_{qs} i_{dr} - \Psi_{ds} i_{qr}) \\ &= \frac{3}{2} p L_m (i_{qs} i_{dr} - i_{ds} i_{qr}) \end{aligned} \quad (3.38)$$

Simulation Block Diagram from the d-q Model of the DFIM For on-line simulation purposes, it is possible to use the d-q model of the DFIM, as illustrated in Figure 3.8 This simulation structure is suitable for implementation in computer based software tools such as Matlab-Simulink. Hence, the simulation block diagram is composed of the following inputs, parameters, and outputs:

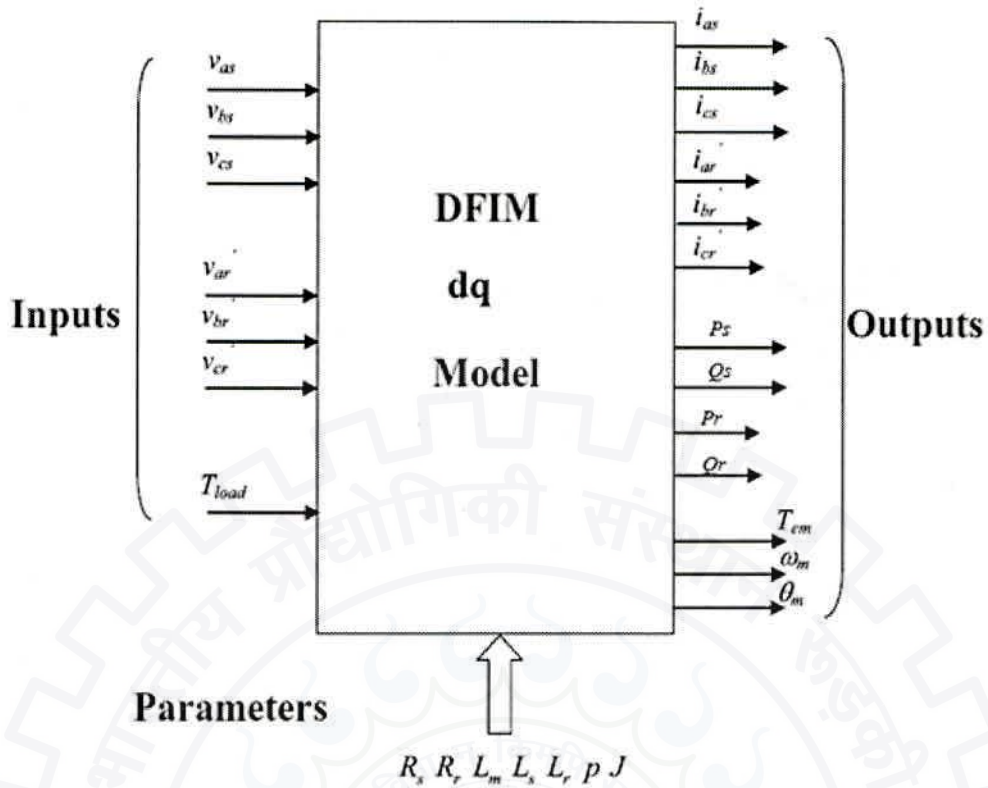


Figure 3.8 Input–output structure of the DFIM simulation block diagram. [76]

- Inputs: Stator and rotor phase (abc) voltages and the load torque T_{load} .
- Parameters: Constant parameters of the DFIM model, including the electric and mechanical parts of the machine.
- Outputs: Stator and rotor phase (abc) currents, stator and rotor Real and Reactive Powers, the electromagnetic torque, the speed, and the rotor angle.

This simulation model calculates the above-mentioned outputs, according to the imposed voltage inputs and the machine's parameters.

After that, the mechanical model of the machine is implemented. In this case, a very simple mechanical model has been considered as depicted in Figure 4.7, mathematically represented by the following equation:

$$T_{em} - T_{load} = J \frac{d\Omega_m}{dt} \quad (3.39)$$

where

J = equivalent inertia of the mechanical axis

T_{load} = external torque applied to the mechanical axis

Ω_m = mechanical rotational speed

From the mechanical model, it is possible to derive the electric rotational speed ω_m and the angle θ_m .

3.1.1.4 STATE-SPACE REPRESENTATION OF DQ MODEL

Continuing with the dynamic model study, a representation of the dq model in state space equations is also possible to obtain. Rearranging Equations (3.28)–(3.31), and taking the fluxes as state-space magnitudes, the model of the DFIM is given by the next expression:

$$\frac{d}{dt} \begin{bmatrix} \vec{\psi}_s^a \\ \vec{\psi}_r^a \end{bmatrix} = \begin{bmatrix} \frac{-R_s}{\sigma L_s} - j\omega_s & \frac{R_s L_m}{\sigma L_s L_r} \\ \frac{R_r L_m}{\sigma L_s L_r} & \frac{-R_r}{\sigma L_r} - j\omega_r \end{bmatrix} \begin{bmatrix} \vec{\psi}_s^a \\ \vec{\psi}_r^a \end{bmatrix} + \begin{bmatrix} \vec{v}_s^a \\ \vec{v}_r^a \end{bmatrix} \quad (3.40)$$

Expanding this last expression in the dq components, we obtain

$$\begin{aligned} \vec{\psi}_s^s &= L_s \vec{i}_s^s + L_m \vec{i}_r^s \\ (\psi_{ds} + j\psi_{qs}) &= L_s (i_{ds} + j i_{qs}) + L_m (i_{dr} + j i_{qr}) \end{aligned} \quad (3.41)$$

Similarly,

$$\begin{aligned} \vec{\psi}_r^r &= L_m \vec{i}_s^r + L_r \vec{i}_r^r \\ (\psi_{dr} + j\psi_{qr}) &= L_m (i_{ds} + j i_{qs}) + L_r (i_{dr} + j i_{qr}) \end{aligned} \quad (3.42)$$

fluxes obtained in dq coordinate

$$\psi_{ds} = L_s i_{ds} + L_m i_{dr} \quad (3.43)$$

$$\psi_{qs} = L_s i_{qs} + L_m i_{qr} \quad (3.44)$$

$$\psi_{dr} = L_m i_{ds} + L_r i_{dr} \quad (3.45)$$

$$\psi_{qr} = L_m i_{qs} + L_s i_{qr} \quad (3.46)$$

Now, state space representation of fluxes

$$\frac{d}{dt} \begin{bmatrix} \psi_{ds} \\ \psi_{qs} \\ \psi_{dr} \\ \psi_{qr} \end{bmatrix} = \begin{bmatrix} -\frac{R_s}{\sigma L_s} & \omega_s & \frac{R_s L_m}{\sigma L_s L_r} & 0 \\ -\omega_s & -\frac{R_s}{\sigma L_s} & 0 & \frac{R_s L_m}{\sigma L_s L_r} \\ \frac{R_r L_m}{\sigma L_s L_r} & 0 & -\frac{R_r}{\sigma L_r} & -\omega_r \\ 0 & \frac{R_r L_m}{\sigma L_s L_r} & -\omega_r & -\frac{R_r}{\sigma L_r} \end{bmatrix} \begin{bmatrix} \psi_{ds} \\ \psi_{qs} \\ \psi_{dr} \\ \psi_{qr} \end{bmatrix} + \begin{bmatrix} v_{ds} \\ v_{qs} \\ v_{dr} \\ v_{qr} \end{bmatrix} \quad (3.47)$$

Once again, if instead of the fluxes the currents are chosen as state-space magnitudes, the equivalent model of the DFIM is expressed as follows, in the synchronous reference frame:

$$\frac{d}{dt} \begin{bmatrix} i_{ds} \\ i_{qs} \\ i_{dr} \\ i_{qr} \end{bmatrix} = \left(\frac{1}{\sigma L_s L_r} \right) \begin{bmatrix} -R_s L_r & \omega_m L_m^2 + \omega_s \sigma L_s L_r & R_r L_m & \omega_m L_m L_r \\ -\omega_m L_m^2 - \omega_s \sigma L_s L_r & -R_s L_r & -\omega_m L_m L_r & R_r L_m \\ R_s L_m & -\omega_m L_s L_m & -R_r L_s & -\omega_m L_r L_s + \omega_s \sigma L_s L_r \\ \omega_m L_s L_m & R_s L_m & \omega_m L_r L_s - \omega_s \sigma L_s L_r & -R_r L_s \end{bmatrix} \begin{bmatrix} i_{ds} \\ i_{qs} \\ i_{dr} \\ i_{qr} \end{bmatrix} + \left(\frac{1}{\sigma L_s L_r} \right) \begin{bmatrix} L_r & 0 & -L_m & 0 \\ 0 & L_r & 0 & -L_m \\ -L_m & 0 & L_r & 0 \\ 0 & -L_m & 0 & L_r \end{bmatrix} \begin{bmatrix} v_{ds} \\ v_{qs} \\ v_{dr} \\ v_{qr} \end{bmatrix} \quad (3.48)$$

CHAPTER:4

SENSORLESS SCHEME OF DOUBLY FED INDUCTION MOTOR DRIVE

4.1 What is Sensorless scheme?

Sensorless means estimation of rotor position and speed without any involvement of any flux terms only with the help of rotor currents in different coordinates and stator and rotor parameters. In high-precision drives, sensor-less scheme is preferred because of the compressed cabling and reduce hardware complexity, increased reliability, lesser cost and low maintenance requirements. There are two major necessities in designing a position and speed sensor-less scheme for doubly fed induction motor drive[24]. Firstly, the Algorithm must enable tracking of rotor position and speed accurately in in all working range of speed. Secondly it should be able to start and function immediately when commanded irrespective of the instant of assigning. It also implies that the initially rotor position need not to be known while commissioning. Generally the sensor-less position and speed estimation schemes can be clustered as open loop and closed loop. A few Model Reference Adaptive Scheme (MRAS) schemes which fall under the closed-loop category require an integrator in the reference model . These schemes differ only in terms of tuning signal driving the adaptation mechanism such as stator flux and rotor flux, stator currents and rotor currents . However, these schemes are sensitive to the variation of the machine parameters. Although the flux estimation is not bothered in closed loop that's why transient performance of the estimator is not satisfactory[37]. A few closed-loop scheme methods employ low-pass filters using certain value of cutoff frequency . A few studies proposed the estimation of the rotor position through the phase comparison of actual and estimated rotor currents and processing the error in a closed loop Proportional Integral (PI) [38]. The estimation of rotor current is based on air gap power vector in whereas a speed-adaptive reduced-order observer is used in . A rotor position phase locked loop is proposed for estimating the rotor speed and position in [39, 40]. The position estimation schemes under open-loop category either used a voltage integrator for flux estimation [31 – 33] or inverse trigonometric function in time domain [34] or

recursive procedures [35 – 38]. Some of them suffer from saturation when they employ the integration stage or at other stages of the process which results in poor performance when the machine runs at a synchronous speed [31 – 33] or influence the machine parameter variations [34]. Flux estimation based on the recursive approach proposed in [35 – 38], In this paper, the authors used a simple and implicit algorithm for estimating the position and speed of the DFIM. Here the rotor position is computed in a direct and implicit manner without the need for computing the stator flux. Particularly, the rotor current components in the stationary reference frame are considered using measured stator quantities. Instead of computing the stator magnetic flux directly or indirectly both, the stator flux terms are substituted with analytical equivalents in terms of computable stator and rotor quantities. Thus, it is an implicit estimation process without computing any flux terms and requires only the measured stator voltage and currents in stator and rotor windings apart from knowledge of the machine parameters. Although it is an open-loop scheme, it does not include any integration, recursive techniques, programmable low-pass filters etc. so this is the main advantage of the sensor less scheme for accurate estimation of speed near synchronous speed, immunity against variation in stator and rotor resistances or in the magnetising inductance Typical simulation work is proposed using Matlab/Simulink .

4.2 Sensorless estimation of rotor position and speed:

Fig. 4a shows the schematic of the implicit position sensorless estimation algorithm. The stator current i_s , the rotor current i_r and the stator voltage v_s , are used for the estimation of rotor position and speed. The three-dimensional distribution of the stator voltage, and the rotor current vectors in different frames of reference are shown in Fig. 4b. The total stator voltage is aligned along the q-axis in the synchronous reference frame (i.e. $v_q = v_s$ and $v_d = 0$). This implies further that the stator magnetizing flux is considered to be aligned in d-axis (in 90 deg. with v_s vector), assuming the no stator resistance.

Also the reference axes for the rotor reference frame are as indicated in Fig. 4b. The rotor current space vector i_r makes an angle θ_1 with respect to the β -axis of stator reference frame and an angle θ_2 with respect to the b -axis of rotor reference frame. Hence, the difference of angles θ_1 and θ_2 gives the rotor position ϵ information.

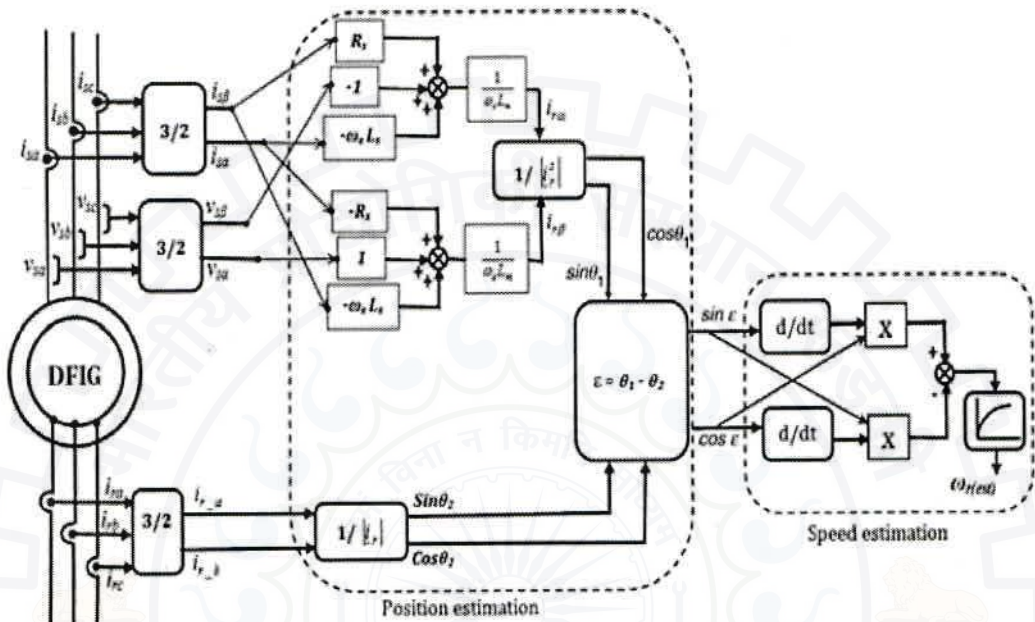


Fig. 4a speed estimation model of DFIM [73]

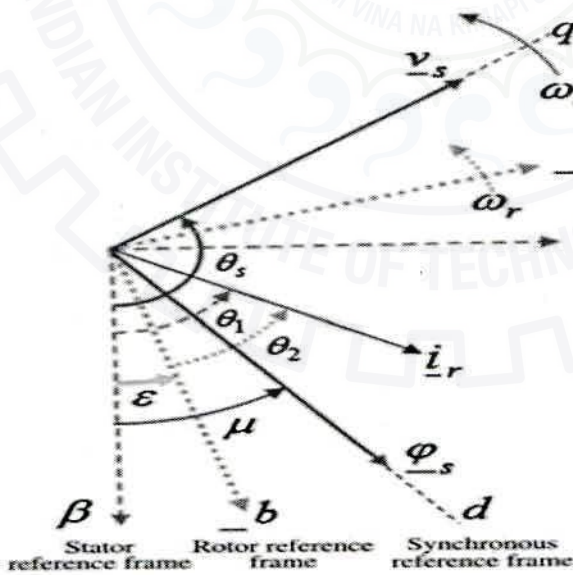


Fig. 4b Representation of rotor current in different coordinates [73]

The whole estimated algorithm is explained by transforming the rotor currents in various reference frame as follows:

1) **Rotor reference frame:** This reference frame is represented by $_{r_a_b}$ coordinates, rotor current i_r is transformed into i_{r_a} and i_{r_b} coordinate which is computed using abc to $_{r_a_b}$ conversion. From fig.4b , we can see that

$$\sin(\theta_2) = \frac{i_{r_a}}{\sqrt{(i_{r_a}^2 + i_{r_b}^2)}} \quad 4.1$$

$$\cos(\theta_2) = \frac{i_{r_b}}{\sqrt{(i_{r_a}^2 + i_{r_b}^2)}} \quad 4.2$$

2) **Stator reference frame:**

Here rotor current coordinates ($i_{r\alpha}$ and $i_{r\beta}$) in stator reference frame can be easily calculated with any computation of stator flux, the stator flux φ . This scheme eliminates the need of stator flux and magnetising current by substitute the value in terms of stator and rotor currents. Stator flux in stationary reference frame is represented by

$$\begin{aligned} \varphi_{s\alpha} &= L_s i_{s\alpha} + L_m i_{r\alpha} \\ \varphi_{s\beta} &= L_s i_{s\beta} + L_m i_{r\beta} \end{aligned} \quad 4.3$$

Rotor current in stationary reference frame is represented as

$$\begin{aligned} i_{r\alpha} &= \frac{(\varphi_{s\alpha} - L_s i_{s\alpha})}{L_m} \\ i_{r\beta} &= \frac{(\varphi_{s\beta} - L_s i_{s\beta})}{L_m} \end{aligned} \quad 4.4$$

Stator voltage in stationary reference frame is represented as

$$\begin{aligned} v_{s\alpha} &= R_s i_{s\alpha} + \frac{d}{dt} \varphi_{s\alpha} \\ v_{s\beta} &= R_s i_{s\beta} + \frac{d}{dt} \varphi_{s\beta} \end{aligned} \quad 4.5$$

The stator magnetising flux Θ_s is along d-axis, which is making angle μ with stationary reference frame and μ is a function of time, the component of stator magnetising flux in stator reference frame is represented as

$$\begin{aligned} \varphi_{s\alpha} &= |\underline{\varphi}_s| \sin(\mu) \\ \varphi_{s\beta} &= |\underline{\varphi}_s| \cos(\mu) \end{aligned} \quad 4.6$$

Differentiate the Equation 4.6, we get

$$\begin{aligned} \frac{d}{dt} \varphi_{s\alpha} &= \frac{d}{dt} [|\underline{\varphi}_s| \sin(\mu)] \\ &= \left[\frac{d}{dt} (\underline{\varphi}_s) \right] \sin(\mu) + |\underline{\varphi}_s| \left[\cos(\mu) \frac{d}{dt} (\mu) \right] \end{aligned}$$

$$\frac{d}{dt} \varphi_{s\alpha} = \left[\frac{d}{dt} |\underline{\varphi}_s| \right] \sin(\mu) + \underline{\varphi}_{s\beta} (\omega_e)$$

$$\begin{aligned} \frac{d}{dt} \varphi_{s\beta} &= \frac{d}{dt} [|\underline{\varphi}_s| \cos(\mu)] \\ &= \left[\frac{d}{dt} (\underline{\varphi}_s) \right] \cos(\mu) + |\underline{\varphi}_s| \left[-\sin(\mu) \frac{d}{dt} (\mu) \right] \end{aligned}$$

$$\frac{d}{dt} \varphi_{s\beta} = \left[\frac{d}{dt} |\underline{\varphi}_s| \right] \cos(\mu) - \varphi_{s\alpha} (\omega_e)$$

Put the above value in Equation 4.5, we get

$$v_{s\alpha} = R_s i_{s\alpha} + \omega_e L_s i_{s\beta} + \omega_e L_m i_{r\beta} \quad 4.7$$

$$v_{s\beta} = R_s i_{s\beta} - \omega_e L_s i_{s\alpha} - \omega_e L_m i_{r\alpha} \quad 4.8$$

After arranging the above terms, we get

$$i_{r\alpha} = \frac{R_s i_{s\beta} - v_{s\beta} - \omega_e L_s i_{s\alpha}}{\omega_e L_m} \quad 4.9$$

$$i_{r\beta} = \frac{v_{s\alpha} - R_s i_{s\alpha} - \omega_e L_s i_{s\beta}}{\omega_e L_m} \quad 4.10$$

$$\frac{d}{dt}(\mu) = \omega_e$$

is the angular velocity of stator magnetising flux, To prevent the variation in stator and grid voltage , we follow inequality

$$\left[\frac{d}{dt} |\underline{\varphi}_s| \right] = \frac{d}{dt} |[L_s i_s + L_m i_r]| \leq \left\{ L_s \frac{d}{dt} [|i_s|] + L_m \frac{d}{dt} [|i_r|] \right\}$$

The only unknown term in the equations from 4.7 to 4.10 is ω_e , which is calculated from the expression given below by referring the figure 4b

$$\sin(\mu) = - \frac{v_{s\beta}}{\sqrt{(v_{s\alpha}^2 + v_{s\beta}^2)}} \quad 4.11$$

$$\cos(\mu) = \frac{v_{s\alpha}}{\sqrt{(v_{s\alpha}^2 + v_{s\beta}^2)}} \quad 4.12$$

$$\omega_e = \cos(\mu) \frac{d}{dt} \sin(\mu) - \sin(\mu) \frac{d}{dt} \cos(\mu)$$

Position of rotor current in stationary reference frame is given as

$$\sin(\theta_1) = \frac{i_{r\alpha}}{\sqrt{(i_{r\alpha}^2 + i_{r\beta}^2)}} \quad 4.13$$

$$\cos(\theta_1) = \frac{i_{r\beta}}{\sqrt{(i_{r\alpha}^2 + i_{r\beta}^2)}} \quad 4.14$$

3) Rotor position estimation:

This is expressed as ($\epsilon = \theta_1 - \theta_2$) which can be obtained from sine and cosine terms.

Rotor position can be computed as from the following expression

$$\begin{aligned} \sin(\epsilon) &= \sin(\theta_1) \cos(\theta_2) - \cos(\theta_1) \sin(\theta_2) \\ \cos(\epsilon) &= \cos(\theta_1) \cos(\theta_2) + \sin(\theta_1) \sin(\theta_2) \end{aligned} \quad 4.15$$

Rotor speed can be estimated using the equation 4.15 as

$$\omega_{r(est)} = \cos(\epsilon) \frac{d}{dt} \sin(\epsilon) - \sin(\epsilon) \frac{d}{dt} \cos(\epsilon)$$

This is the expression for the sensorless speed estimation of doubly fed induction machine, if any differential terms contribute the noise this can be eliminated by using low pass filter.

4.3 ADVANTAGE OF SENSORLESS SCHEME

- ❖ Reduced cabling
- ❖ Reduced hardware complexity
- ❖ Increased reliability
- ❖ Less maintenance required
- ❖ Lesser cost of the machine
- ❖ Better noise immunity
- ❖ Hostile environment
- ❖ Fluctuation in grid voltage and frequency can be easily restricted

4.4 APPLICATION OF SENSORLESS SCHEME

- ❖ It can be used in explosive and hazardous environment like mines, contaminated environment, nuclear power plant, underground and underwater
- ❖ It can also be used in domestic appliances like air conditioning, refrigerator, conveyor, blower etc.

Sensorless scheme is preferred in above devices because in such places if speed sensor is connected on the rotor shaft for speed measurement then during measurement under such hazardous environment there could be a problem to person safety or inaccurate reading measurement due to vibration in the shaft so it is better to choose sensorless scheme. This scheme automatically measures the speed at a certain distance from shaft

CHAPTER-5

SIMULATION RESULT

5.1 Performance of DFIM model under Sensorless Scheme

The performance evaluation of sensorless scheme of doubly fed induction machine drive has been simulated on MATLAB. The circuit parameters used for machine modeling and execution of the sensorless scheme given in the Table 1. As shown in the Fig 5.1, whole simulation model of DFIM along with sensorless scheme is presented.

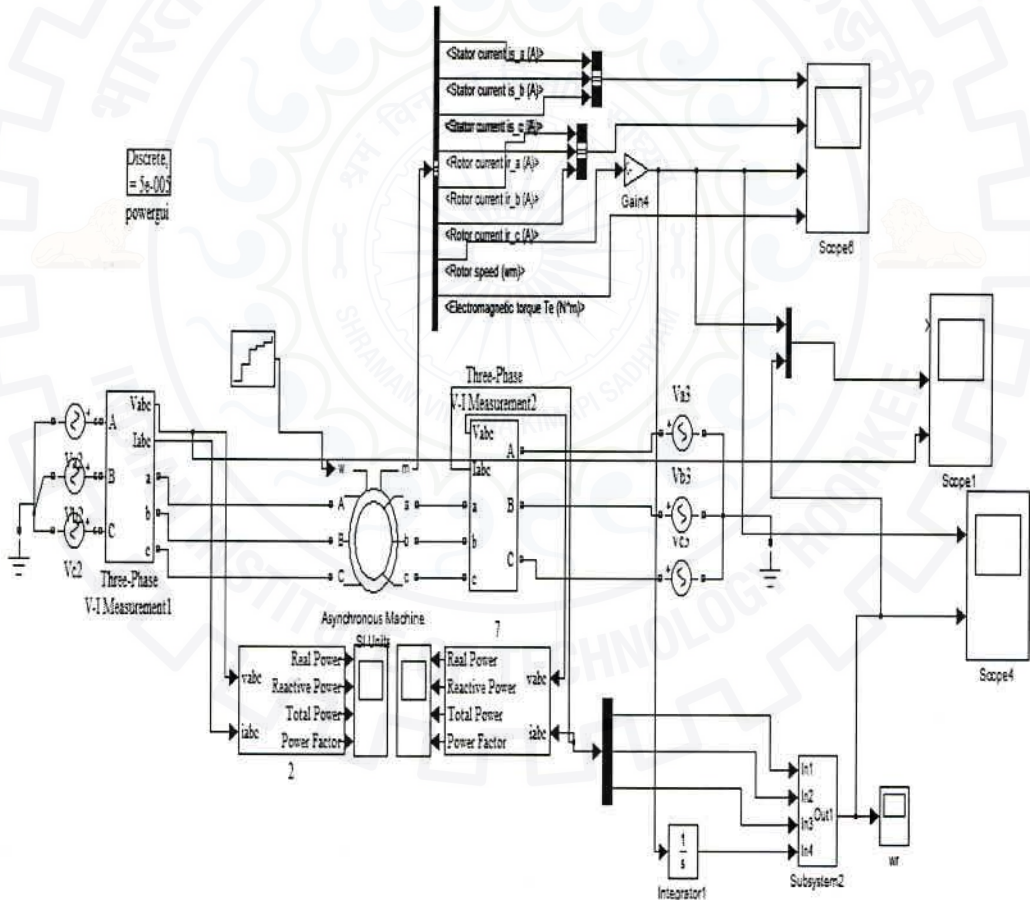


Fig 5.1 Simulation model of doubly fed induction machine

5.2 Circuit Parameters

Table 1 shows the circuit parameters used in DFIM

CIRCUIT PARAMETERS	VALUE
Rated power	3 Hp
Stator voltage (star connected)	415V
Rotor voltage (star connected)	185V
Stator current	4.7A
Rotor current	7.5A
Stator resistance(ohm)	4.43
Stator inductance(mH)	0.02571
Rotor resistance(ohm)	3.51
Rotor inductance(mH)	0.02571
No. of pole pair	2
Magnetizing inductance(mH)	0.2975

5.3 Various operations of the DFIM:

a) Machine under sub synchronous mode:

Initially the machine is running at 1480 rpm which is quite close to synchronous speed i.e 1500rpm .But after a certain a time at $t= 2$ sec, speed decreases to 1000 rpm still machine is running in subsynchronous mode or motoring mode and $t=4$ second

machine further attains its original speed of 1480 rpm. The corresponding curves are shown in Fig 5.3(a) which shows the comparison of reference and estimated rotor speed. The maximum percentage error between reference and estimated rotor speed during the various transient periods is given in Table 2.

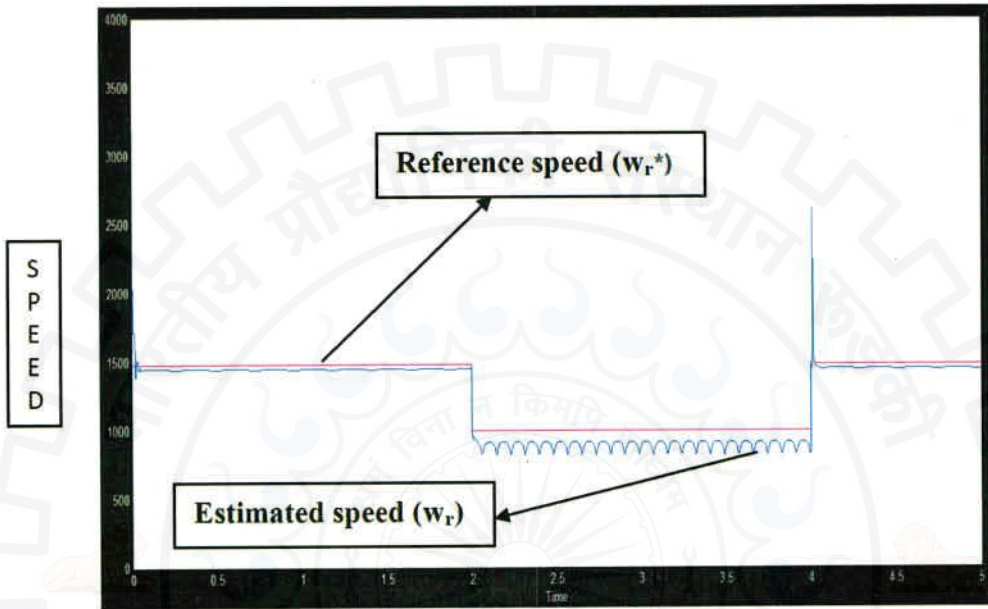


Fig 5.3(a) Performance of machine under subsynchronous speed and comparison of reference and estimated rotor speed

b) Machine under supersynchronous mode:

Initially the machine is running at 1480 rpm which is quite close to synchronous speed i.e 1500rpm .But after a certain a time at $t= 2$ sec, speed increases to 1600 rpm which shows machine is running in supersynchronous mode or generating mode and $t= 4$ second, machine further attains its original speed of 1480rpm . The corresponding curves are shown in Fig 5.3(b) which shows the comparison of reference and estimated rotor speed. The maximum percentage error between reference and estimated rotor speed during the various transient periods is given in Table 2.

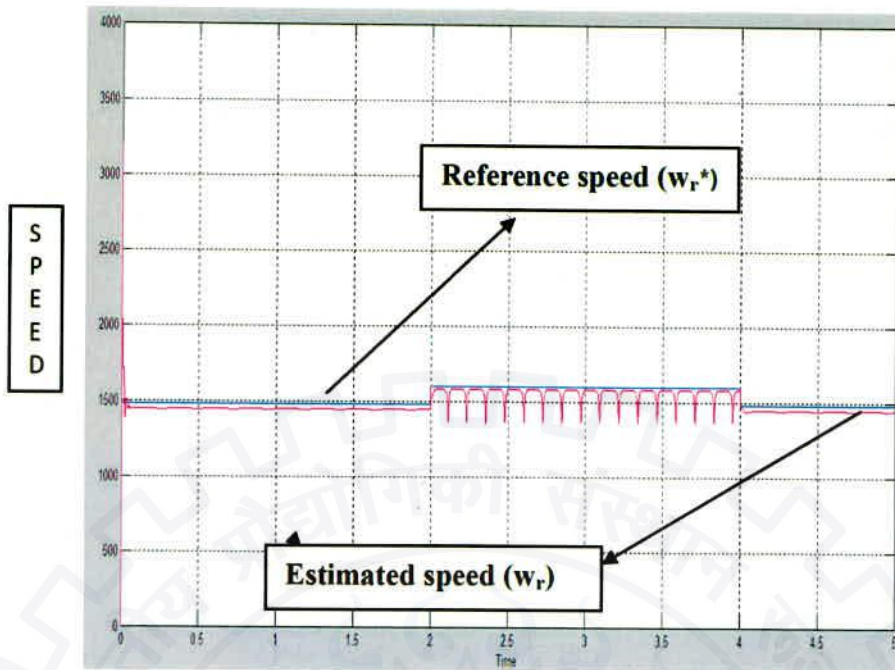


Fig 5.3(b) Performance of machine under supersynchronous speed and comparison of reference and estimated rotor speed

5.4 Maximum error between reference and estimated rotor speed measurements

As shown in Fig.5a and Fig.5b, Estimated speed is little bit different from reference speed so this difference is measured in terms of percentage error, we have to approach to make this error as small as possible. This is all shown in Table 2

Operating conditions	Maximum %error between reference(w_r^*) and estimated speed(w_r)
1) Subsynchronous mode	
a) Upto 2 seconds, Reference speed=1480rpm and estimated speed= 1450rpm	$(1480-1450)*100/1480$ = 2.01%
b) For next 2 seconds, Reference speed=1000rpm and estimated speed=980rpm	$(1000-980)*100/1000$ = 2%

2) Super synchronous mode	
a) Upto 2 seconds, Reference speed= 1480rpm and estimated speed=1450rpm	$(1480-1450)*100/1480$ = 2.01%
b) For the next 2 seconds, reference speed=1600rpm and estimated speed= 1580rpm	$(1600-1580)*100/1600$ = 1.25%

The max error generated in above two cases is 2% which is acceptable that employ estimated speed is approximately equal to reference speed.

CHAPTER :6

INDUCTION MOTOR UNDER SENSOR FAULT

6.1 Introduction

In this chapter, we will discuss how the system performance will be assessed after injecting the fault at speed sensor. Fault is injected into the model in sequential levels and the system performance is assessed after each fault. An induction motor drive requires measurements of the three-phase currents, torque and speed. We will see how the system performance is changing under different load conditions after the fault injection at the speed sensor [59]. This is one of the best examples to show how a sensorless scheme can be a better option for induction motor drive.

6.2 Types of fault injected at speed sensor

The set of faults injected at the speed sensor are

- ❖ omission
- ❖ gain
- ❖ constant

Omission is modeled by setting the sensor output to zero. Gain is modeled by applying a numerical gain to the sensor signal, where the sensor output is amplified or attenuated due to an internal fault or due to a fault in its interface circuitry [70]. A sensor could also get stuck at a constant value if the interface circuit fails or saturates, e.g., the saturation of a magnetic core or a ground wire break.

6.3 Performance evaluation:

Since the simulation model was validated under faults, all faults were injected into the model and the system response was monitored. In each case, a fault is injected at $t=5\text{sec}$ and performance is analyzed, how the speed, current, torque are affected.

1) Omission:

This type of fault is injected at the speed sensor of the induction motor drive. Before fault injection, we can see that the speed is set at 120 rad/sec. But as the fault is injected at

t=5seconds, During no load condition speed reduces to 40 rad/sec and the current enhances up as shown in Fig6.1, Similarly in case of half load condition, speed further reduces as fault is injected at t=10sec and current level increases up to 135 ampere which is quite sufficient to damage the machine and torque also increases tremendously to 250NM which is quite sufficient to damage the machine as shown in fig6.2. Similarly we can analyse the same performance during full load condition as shown in fig.6.3

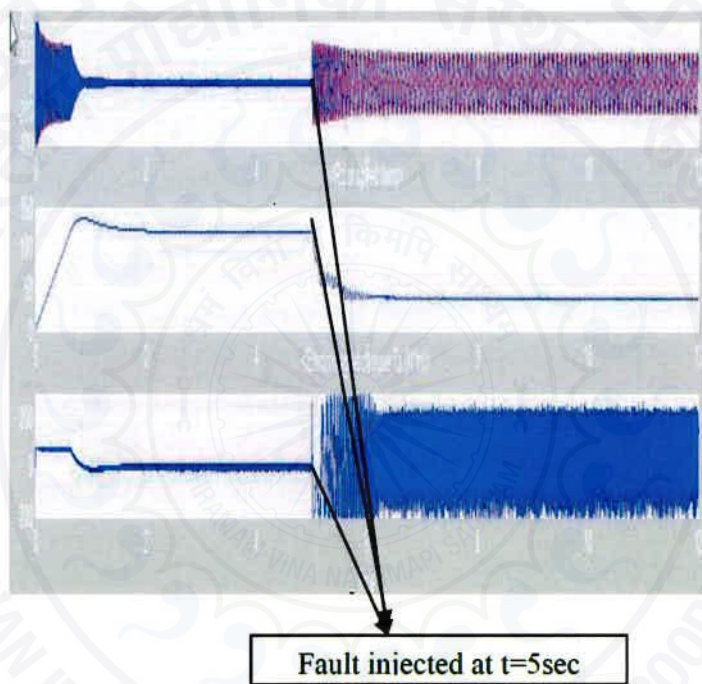


Fig. 6.1: No load performance of induction motor under Omission Fault Injection at t=5sec

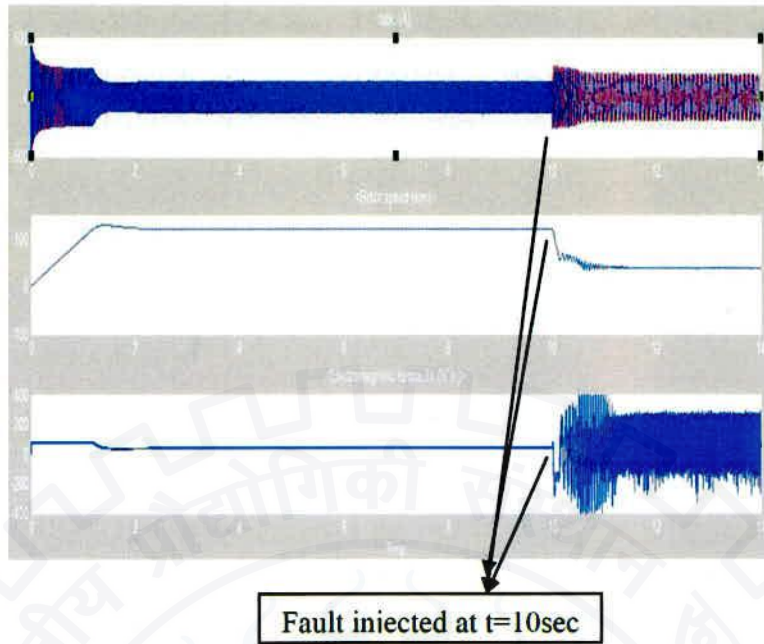


Fig6.2. Half load performance of induction motor under omission fault Injection at t=10sec

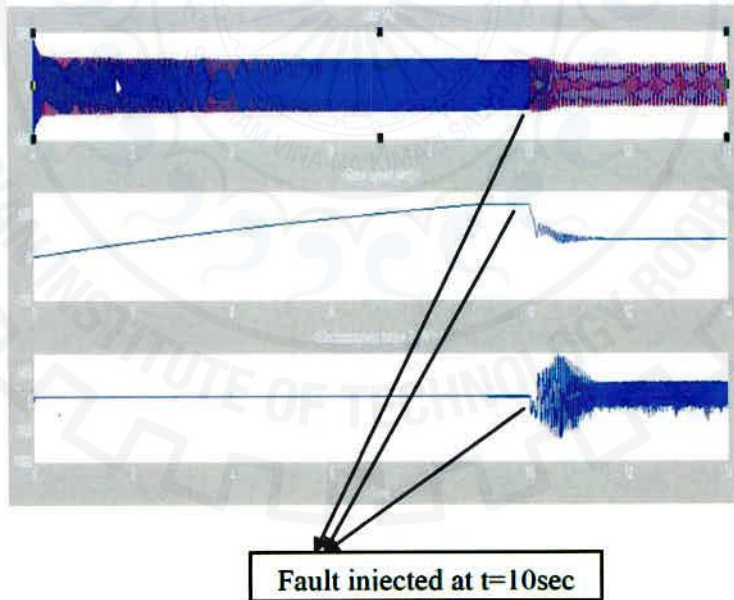


Fig.6.3 Full load performance of induction motor under Omission Fault Injection at t=10sec

2) Gain (1.5)

This type of performance can be seen in fig.6.4 we can see that during half load condition speed was set at 120 rad/sec and after the gain fault injection it increases to 150 rad/sec and the current level increases up from 100 to 200 amperes and torque increases from 40 to 150 NM. induction motor . This increment in current and torque which is 2-3 times the original value is sufficient to deteriorate the machine

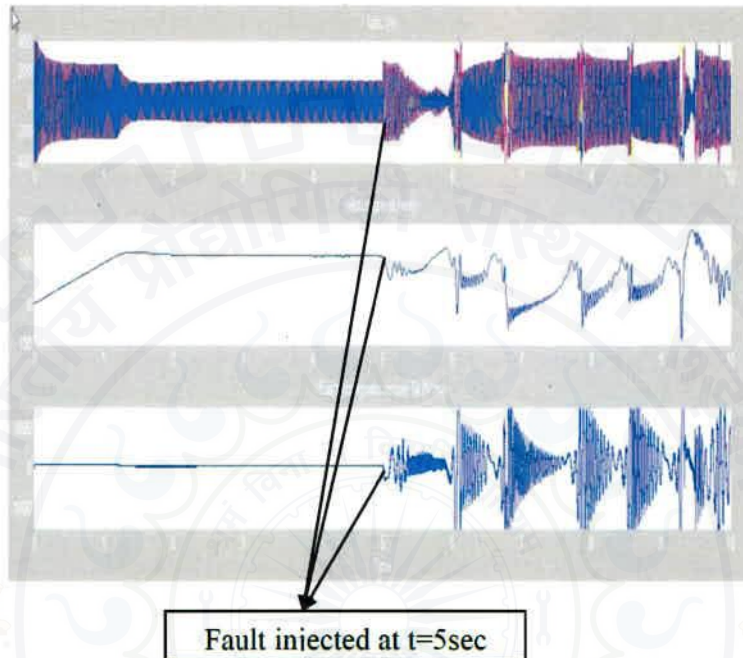


Fig6.4 Half load performance of induction motor drive under gain Fault Injection at t=5sec

6.4 CONCLUSION:

As shown from the Fig6.1 to Fig6.4, when fault occur on the speed sensor there is drastic change in the value of speed, current and torque which could deteriorate the machine or disturbed all the characteristic of the machine .If we use sensorless scheme for the estimation of the speed, then no such type of above problem related to fault injection will occur because as name suggest sensorless 'means' removal of speed sensor and speed is estimated through current sensor and other circuit parameters. It means no speed sensor, no possibility of fault occurrence on speed sensor which automatically increases the reliability, efficiency of machine which simply shows sensorless scheme is quite advantageous for above type of cases.

MOTOR PARAMETER	VALUES
RATED POWER	50 HP
RATED SPEED	120 RAD/SEC
NO. OF POLES	2
STATOR RESISTANCE(R_s)	0.087
STATOR LEAKAGE INDUCTANCE(L_s)	0.8e-3
ROTOR LEAKAGE INDUCTANCE(L_r)	0.8e-3
MAGNETISING INDUCTANCE(L_m)	34.7e-3
ROTOR RESISTANCE(R_r)	0.228
INERTIA (J)	1.662
RATED VOLTAGE(L-L)	460V
External rotor resistance for wound rotor	3

CHAPTER 7:

CONCLUSION AND FUTURE SCOPE OF THE WORK

7.1 CONCLUSION

A simple and implicit sensorless scheme has come introduced for the first time in this study. The method of computation is based on substitutions of equivalent terms (which is derived from basics) for d,q components of stator magnetizing flux in the stationary reference frame. Basically this stator magnetizing flux is eliminated by substituting in terms of stator current, stator inductance, stator resistance, through this way speed can be easily estimated without any computation of stator or rotor flux, that is the main motto of sensorless scheme. The remarkable simplicity and the effectiveness of the estimator have been demonstrated through numerical analysis. We operate the DFIM in both subsynchronous and supersynchronous mode and estimate the sensorless speed, As the figure 5.3(a) and 5.3(b) shows that estimated speed is somewhat close to reference speed but there is some error generating in it. The maximum error in speed estimation is observed around 2.1% which is somewhat acceptable or we can say that estimated rotor speed is tending close to reference rotor speed. Simulation results of the excellent drive performance at different speeds of operation (subsynchronous, supersynchronous and synchronous speed) are illustrated.

(The proposed estimation algorithm can also be employed in the power control of grid connected induction generator for wind power applications)

7.2 FUTURE SCOPE THE WORK

As we seen in the chapter 6, we analyze the performance of 3 phase induction motor under the various fault injected at speed sensor. The fault occurrence on the speed sensor will drastically change the characteristics of the machine like speed, torque, current etc. under the different loading conditions. We know that as load increases current drawn from the source increases and speed decreases, same phenomenon will occur if fault occur on speed sensor, there is abrupt change in circuit parameters.

As seen from the fig 6.1 to 6.4 machine is responding differently under different loading conditions because as fault took place on speed sensor current increases up, and it may exceeds its rated value and speed decreases to a very low value all these problems are sufficient to destroy the machine so to overcome the above problem we prefers sensor less scheme, if there is no speed sensor, no such type of above fault will occur. If we want to do same type of thing in DFIM, that is our future work so we need to design a whole model of DFIM along with sensors and design the sensor less scheme and will observe that how could fault occurrence on speed sensor be prevented . This analysis could be more useful to wind power application or hazardous environment like coal mines etc. where speed is estimated through shaft connected speed sensor, for human safety and better machine performance, sensor less estimation of speed is preferred.

REFERENCES

- [1] Jiang.J and .Holtz.J, High Dynamic speed sensorless AC drive with On-line model parameter turning for steady state accuracy, IN I.E.E.E. Trans. On Industrial Elec., Vol.44, No.2, April. 1997
- [2] Holtz J. Speed estimation and sensorless control of AC drives, Proc. 19th Intl. conf. on Ind. Elec., Nov, 1993.
- [3] Kanmachi T and Takahasahi I, Sensorless speed control of an Induction motor, IEEE Industrial Application. Magazine, Vol.1, Jan.-Feb., (1995)
- [4] Tamai S, Sugimoto H and Yano M, Speed sensorless vector control of Induction motor with model reference adaptive system, Conf. Rec. IEEE/IAS annual meeting, 1987.
- [5] Al-Tayie J. K. and Acarnely P. P. Estimation of speed, stator temperature and rotor temperature in cage IM drive using the extended Kalman filter algorithm, IEEE Proc. Elect. Power applications., Vol.144, No5, Sep, 1998.
- [6] Schauder C, Adaptive speed identification for vector control of IM without rotational transducers, Conf. rec. IEEE/IAS annual meeting, 1989.
- [7] Zibai Xu, On Line speed estimation of induction motors", M.S. Thesis, Univ. of New Orleans, 1995.
- [8] Pradhyumnan R. Real-Time DSP Implementation of Motor Current Signature Analysis for Induction motor Speed Estimation and Control, M.S. Thesis, Clarkson University, 1997.
- [9] Williams B, .Goodfellow J and Green T. Sensorless speed measurement of inverter driven squirrel cage induction motors, in Proc. IEE 4th Int. Conf. On Power Electronic and Variable Speed Drives, 1990.
- [10]. HOPFENSBERGER, B.—ATKINSON, D.—LAKIN,R. A.: Stator Flux Oriented Control of a Cascaded Doubly-Fed Induction Machine, IEE Proc. Electr. Power Appl. 146 No. 6 (Nov 1999), 597–605.

- [11] Blasco R, Asher G.M., Bradley K.J. and Summer M. Performance of FFT-rotor slot harmonic speed detector for sensorless induction motor drives, IEE, Power App., Vol.143, No.3, pp.258-268,(1996)
- [12] Hurst K.D., Habetler T.G. Sensorless speed measurement using current harmonic spectral estimation on induction motor drives, IEEE Trans. on power electronics, Vol.11, No.1, pp.66-73,(1996).
- [13] Hurst K.D, Habetler T.G, Griva G and Profumo F. Speed sensorless field oriented control of IM using current harmonic spectral estimation, Conf. Rec. IEEE/ IAS annual meeting, pp.601-607,(1994)
- [14] Danish Wind Industry Association, Guided Tour on Wind energy, available from <http://www.windpower.org/en/tour/>.
- [15] Landau Y.D Adaptive Control –The Model Reference Approach”, Marcel Dekker Inc., New York, 1979
- [16] Chee-Mun Ong. Dynamic simulation of Electric machinery—using MATLAB/SIMULINK , Prentice Hall, New Jersey, 1998
- [17] Nise Norman S. Control System Engineering”, Addison-Wesley publishing company, California, 1995
- [18] Muller, S., Deicke, M., De Doncker, R.W.: ‘Doubly fed induction generator systems for wind turbines’, IEEE Ind. Appl. Mag., 2002, 8,(3), pp. 26–33
- [19] Yamamoto, M., Motoyoshi, O.: ‘Active and reactive power control for doubly-fed wound rotor induction generator’, IEEE Trans. Power Electronics, 1991, 6, (4), pp. 624–629
- [20] Cardenas, R., Pena, R., Clare, J.C., Asher, G.M., Probst, J.: ‘MRAS observers for sensorless control of doubly-fed induction generators’, IEEE Trans. Power Electron., 2008, 23, (3), pp. 1075–1084

- [21] Maiti, S., Chakraborty, C.: 'A new instantaneous reactive power based MRAS for sensorless induction motor drive', *Simulation Model. Practical Theory*, 2010, 18, (9), pp. 1314–1326
- [22] Kojabadi, H.M.: 'Active power and MRAS based rotor resistance identification of an IM drive', *Simulation Model. Practical Theory*, 2009, 17, (2), pp. 376–389
- [23] Comanescu, M., Xu, L.: 'An improved flux observer based on PLL frequency estimator for sensorless vector control of induction motors', *IEEE Trans. Ind. Electron.*, 2006, 53, (1), pp. 50–56
- [24] Marques, G.D, Pires, V.F., Sousa, S., Sousa, D.M.: 'A DFIG sensorless rotor-position detector based on a hysteresis controller', *IEEE Trans. Energy. Convertors.*, 2011, 26, (1), pp. 9–17
- [25] Yang, S., Ajjarapu, V.: 'A speed-adaptive reduced-order observer for sensorless vector control of doubly fed induction generator-based variable-speed wind turbines', *IEEE Trans. Energy Convertors.*, 2010, 25, (3), pp. 891–900
- [26] Mwinyiwiwa, B., Zhang, Y., Shen, B., Ooi, B.-T.: 'Rotor position phase-locked loop for decoupled P-Q control of DFIG for wind power generation', *IEEE Trans. Energy. Convertors.*, 2009, 24, (3), pp. 758–765
- [27] Shen, B., Mwinyiwiwa, B., Zhang, Y., Ooi, B.-T.: 'Sensorless maximum power point tracking of wind by DFIG using rotor position phase lock loop (PLL)', *IEEE Trans. Power Electron.*, 2009, 24, (4), pp. 942–951
- [28] Xu, L., Cheng, W.: 'Torque and reactive power control of a doubly fed induction machine by position sensorless scheme', *IEEE Trans. Ind. Application*, 1995, 31, pp. 636–642
- [29] Hopfensperger, B, Atkinson, D.J., Lakin, R.A.: 'Stator-flux-oriented control of a doubly-fed induction machine with and without position encoder', *IEE Proc. Electr. Power Appl.*, 2000, 147, (4), pp. 241–250

- [30] Bogalecka, E.: 'Power control of a double fed induction generator without speed or position sensor'. Conference on Record EPE, vol. 377, part 8, chapter 50, pp. 224–228
- [31] Morel, L., Godfroid, H., Mirzaian, A., Kauffmann, J.M.: 'Double-fed induction machine: converter optimization and field oriented control without position sensor', IEE Proc. Electronics Power Appl., 1998, 145, pp. 360–368
- [32] Abolhassani, M., Enjeti, P., Toliyat, H.: 'Integrated doubly fed electric alternator/active filter (IDEA), a viable power quality solution, for wind energy conversion systems', IEEE Trans. Energy Convertors., 2008, 23, (2), pp. 642–650
- [33] Jain, A.K., Ranganathan, V.T.: 'Wound rotor induction generator with sensorless control and integrated active filter for feeding nonlinear loads in a stand-alone grid', IEEE Trans. Ind. Electron., 2008, 55, (1), pp. 218–228
- [34] Datta, R., Ranganathan, V.T.: 'A simple position-sensorless algorithm for rotor-side field-oriented control of wound-rotor induction machine', IEEE Trans. Ind. Electron., 2001, 48, (4), pp. 786–793
- [35] Datta, R., Ranganathan, V.T.: 'Decoupled control of active and reactive power for a grid-connected doubly-fed wound rotor induction machine without position sensors'. Proc. Conference. on Rec. IEEE/IAS Annual Meeting, 1999, pp. 2623–2630
- [36] Leonhard, W.: 'Control of electrical drives' (Springer-Verlag, Berlin, Germany, 2003, 3rd edn.)
- [37] Krause, P.C., Wasynczuk, O., Sudhoff, S.D.: 'Analysis of electric machinery and drive systems' (Wiley-Interscience, USA, 2002)
- [38] Vas, P.: 'Sensorless vector and direct torque control' (Oxford University Press, London, UK, 1998)
- [39] Pena, R., Clare, J.C., Asher, G.M.: 'A doubly fed induction generator using back-to-back PWM converters and its application to variable-speed wind-energy generation', IEE Proc. Electr. Power Appl., 1996, 143, (5), pp. 231–241

- [40] Yao, J., Li, H., Liao, Y., Chen, Z.: 'An improved control strategy of limiting the DC-link voltage fluctuation for a doubly fed induction wind generator', IEEE Trans. Power Electron., 2008, 23, (3), pp. 1205–1213
- [41] [Online]. Available: <http://www.wired.com/thisdayintech/2009/12/1204gm-ev1-electric-car/>
- [42] [Online]. Available:<http://www.teslamotors.com/roadster/technology/motor,2011>
- [43] A. M. Bazzi, A. D. Dominguez-Garcia, and P. T. Krein, "A method for impact assessment of faults on the performance of field-oriented control drives: A first step to reliability modeling," in Proc. IEEE Appl. Power Electron. Conf. Expo., 2010, pp. 256–263.
- [44] M. Rausand and A. Høyland, System Reliability Theory: Models, Statistical Methods, and Applications, 2nd ed. Hoboken, NJ: Wiley, 2005.
- [45] D. Kastha and B. K. Bose, "Investigation of fault modes of voltage-fed inverter system for induction motor drive," IEEE Trans. Ind. Appl., vol. 30, no. 4, pp. 1028–1038, Jul./Aug. 1994.
- [46] J. Pontt, J. Rodriguez, J. Rebolledo, L. S. Martin, E. Cid, and G. Figueroa, "High-power LCI grinding mill drive under faulty conditions," in Proc. Ind. Appl. Conf., 2005, pp. 670–673.
- [47] R. M. Tallam, D. W. Schlegel, and F. L. Hoadley, "Failure mode for ac drives on high resistance grounded systems," in Proc. IEEE Appl. Power Electron. Conf. Expo., 2006, pp. 1587–1591.
- [48] Y. Yuexin and A. Y. Wu, "Transient response of electric drives under utility upset conditions," in Proc. Pulp Paper Ind. Tech. Conf., 1996, pp. 77–85.
- [49] BANSAL, R. C.—BHATTI, T. S.—KOTHARI, D. P. : Bibliography on the Applications of Induction Generators in Non-Conventional Energy Systems, IEEE Transactions on Energy Conversion 18 No. 3 (Sep 2003), 433–439.

- [50] A. Fekih and F. N. Chowdhury, "A fault tolerant control design for induction motors," in Proc. IEEE International Conference. Syst., Man Cybern., 2005, pp. 1320–1325.
- [51] S. Green, D. J. Atkinson, A. G. Jack, B. C. Mecrow, and A. King, "Sensorless operation of a fault tolerant PM drive," IEE Proc. Elect. Power Appl., vol. 150, no. 2, pp. 117–125, Mar. 2003.
- [52] O. Jasim, C. Gerada, M. Sumner, and J. Arellano-Padilla, "Investigation of induction machine phase open circuit faults using a simplified equivalent circuit model," in Proc. Int. Conf. Elect. Mach., 2008, pp. 1–6.
- [53] K. S. Lee and J. S. Ryu, "Instrument fault detection and compensation scheme for direct torque controlled induction motor drives," IEE Proc. Control Theory Appl., vol. 150, no. 4, pp. 376–382, Jul. 2003.
- [54] O. Ondel, G. Clerc, E. Boutleux, and E. Blanco, "Fault detection and diagnosis in a set "Inverter-induction machine" through multidimensional membership function and pattern recognition," IEEE Trans. Energy Convers., vol. 24, no. 2, pp. 431–441, Jun. 2009.
- [55] R. L. A. Ribeiro, C. B. Jacobina, E. R. C. Da Silva, and A. M. N. Lima, "Compensation strategies in the PWM-VSI topology for a fault tolerant induction motor drive system," in Proc. IEEE Int. Symp. Diagnost. Electrical Machine, Power Electronics. Drives, 2003, pp. 211–216.
- [56] R. B. Sepe, Jr., B. Fahimi, C. Morrison, and J. M. Miller, "Fault tolerant operation of induction motor drives with automatic controller reconfiguration," in Proc. IEEE Int. Elect. Mach. Drives Conf., 2001, pp. 156–162.
- [57] W. G. Zanardelli, E. G. Strangas, and S. Aviyente, "Identification of intermittent electrical and mechanical faults in permanent-magnet ac drives based on time-frequency analysis," IEEE Trans. Ind. Appl., vol. 43, no. 4, pp. 971–980, Jul./Aug. 2007.

- [58] M. T. Abolhassani and H. A. Toliyat, "Fault tolerant permanent magnet motor drives for electric vehicles," in Proc. IEEE Int. Elect. Mach. Drives Conf., 2009, pp. 1146–1152.
- [59] J. C. Salmon and B. W. Williams, "A split-wound induction motor design to improve the reliability of PWM inverter drives," IEEE Trans. Ind. Appl., vol. 26, no. 6, pp. 143–150, Jan./Feb. 1990.
- [60] J. W. Bennett, A. G. Jack, B. C. Mecrow, D. J. Atkinson, C. Sewell, and G. Mason, "Fault-tolerant control architecture for an electrical actuator," in Proc. IEEE Power Electron. Spec. Conf., 2004, pp. 4371–4377.
- [61] O. Wallmark, L. Harnefors, and O. Carlson, "Control algorithms for a fault-tolerant PMSM drive," IEEE Trans. Ind. Electron., vol. 54, no. 4, pp. 1973–1980, Aug. 2007.
- [62] A. W. Williams, "High reliability 3-phase variable-frequency inverter," IEEE Proc. Electr. Power Appl., vol. 129, no. 6, pp. 353–354, Nov. 1982.
- [63] S. Bolognani, L. Peretti, L. Sgarbossa, and M. Zigliotto, "Improvements in power line communication reliability for electric drives by random PWM techniques," in Proc. IEEE Ind. Electron. Conf., 2006, pp. 2307–2312.
- [64] G. F. D'Addio, S. Savio, and P. Firpo, "Optimized reliability centered maintenance of vehicles electrical drives for high speed railway applications," in Proc. IEEE Int. Symp. Ind. Electron., 1997, vol. 2, pp. 555–560.
- [65] F. A. DeWinter, R. Paes, R. Vermaas, and C. Gilks, "Maximizing large drive availability," IEEE Ind. Appl. Mag., vol. 8, no. 4, pp. 66–75, Jul./Aug. 2002.
- [66] J. A. Oliver and D. Poteet, "High-speed, high-horsepower electric motors for pipeline compressors: Available ASD technology, reliability, harmonic control," IEEE Trans. Energy Convers., vol. 10, no. 3, pp. 470–476, Sep. 1995.
- [67] R. Bozzo, V. Fazio, and S. Savio, "Power electronics reliability and stochastic performances of innovative ac traction drives: A comparative analysis," in Proc. IEEE Power Tech. Conf., 2003, p. 7.

- [68] R. D. Klug and M. Griggs, "Reliability and availability of megawatt drive concepts," in Proc. Int. Conf. Power Syst. Tech., 2004, pp. 665–671.
- [69] P. Wikstrom, L. A. Terens, and H. Kobi, "Reliability, availability, and maintainability of high-power variable-speed drive systems," IEEE Trans. Ind. Appl., vol. 36, no. 1, pp. 231–241, Jan./Feb. 2000.
- [70] Ali M. Bazzi, Alejandro Dominguez –Garcia, "Markov reliability modeling for induction motor drives under field oriented control" IEEE transactions on power electronics , vol.27,No.2, February 2012
- [71] M. H. J. Bollen and P. M. E. Dirix, "Simple model for post-fault motor behaviour for reliability/ power quality assessment of industrial power systems," IEEE Proc. Generation, Transmission. Distribution, vol. 143, no. 1, pp. 56–60, Jan. 1996.
- [72] M. Molaei, H. Oraee, and M. Fotuhi- Firuzabad, "Markov model of drive motor systems for reliability calculation," in Proc. IEEE Int. Symp. Ind. Electron., 2006, pp. 2286–2291.
- [73] A. Karthikeyan , C. Nagamani and Aritra Basu Ray Chaudhury, "An Implicit sensorless position / speed estimator for the speed control of a Doubly Fed Induction Motor," Department of Electrical and Electronics Engineering , National Institute of Technology Tiruchirappalli , India , IEEE PES Innovative Smart Grid Technologies, India.
- [74] S.A. Gomez and J.L.R Amenendo , "Grid Synchronization of Doubly Fed Induction Generators Using Direct Torque Control, " in Proc. IEEE IECON 2002 Conference 2002
- [75] Gonzalo Abad, Jesus Lo'pez, Miguel A. Rodríguez, Louis Marroyo, Grzegorz Iwanski, "Doubly Fed Induction Machine Modeling and Control for Wind Energy Generation, " IEEE Press , John Wiley & Sons , Inc. , Publisher , pp. 209-234.
- [76] Petersson . A. , "Analysis , Modeling , and Control of Doubly-Fed Induction Generators for Wind Turbines, " Ph.D Chalmers University

of Technology, Sweden.



APPENDIX

Doubly fed induction machine:

3 Hp, 415V, 50Hz, 3 phase ; Stator: 415V, Y connected, 4.7A;

Rotor: 185V, Y connected 7.5A.

Stator

Rotor

Resistance $R_s = 4.43 \Omega$

Resistance $R_r = 3.51 \Omega$

Inductance $L_s = 25.82 \text{ mH}$

Inductance $L_r = 25.82 \text{ mH}$

Magnetising Inductance $L_m = 0.2975 \text{ H}$

Magnetizing Inductance $L_o = 281.95 \text{ mH}$